https://dx.doi.org/10.1016/j.tra.2020.03.035

A MULTI-MODAL NETWORK EQUILIBRIUM MODEL WITH CAPTIVE MODE CHOICE AND PATH SIZE LOGIT ROUTE CHOICE

Guangchao Wang
Assistant Professor
School of Information Management, Central China Normal University, Wuhan, Hubei, 430079, P.R. China

Anthony Chen
Professor
Corresponding Author
Department of Civil and Environmental Engineering, The Hong Kong Polytechnic University, Hung Hom, Kowloon, Hong Kong
Email: anthony.chen@polyu.edu.hk

Songyot Kitthamkesorn
Faculty Member
Excellence Center in Infrastructure Technology and Transportation Engineering (ExCITE)
Department of Civil Engineering, Chiang Mai University, Chiang Mai, Thailand

Seungkyu Ryu
Post-doctoral Student
Korea Institute of Science Technology and Information, Dajeon, Korea

Hang Qi
Assistant Professor
Institute for Advanced Studies in Finance and Economics, Hubei University of Economics, Wuhan, 430000, P.R. China

Ziqi Song
Assistant Professor
Department of Civil and Environmental Engineering, Utah State University, Logan, UT 84322, United States

Jianguo Song

School of Information Management, Wuhan University, Wuhan, 43000, P.R. China

ABSTRACT

In this paper, we consider captive mode travelers (those who have no other choices but rely on one specific travel mode for daily commuting trips) in a multi-modal network equilibrium (MMNE) problem. Specifically, the dogit model is adopted to account for captive mode travelers in the modal split problem, and the path-size logit (PSL) model is used to capture route overlapping effects in the traffic assignment problem. The dogit-PSL MMNE model is formulated as an equivalent entropy-based mathematical programming (MP) problem, which admits solution existence and uniqueness. Three numerical examples are provided. The first example examines the effects of mode captivity and route overlapping on network performances and observes that accounting for captive mode travelers would produce different equilibrium states and hence the network performance indicators. The second example applies the dogit-PSL MMNE model for evaluating the exclusive bus lane (EBL) expansion plans, in which a consistent synthetic proportional index is proposed. Numerical results show that considering mode captivity may cause substantial differences (up to 50 percent of odds in the given scenarios) in EBL line expansion decisions. The third example implements the dogit-PSL MMNE model in the Seoul network to show the applicability of the dogit-PSL MMNE model in a real-size multi-modal system.

Keywords*:* Captive mode traveler; dogit model; multi-modal network equilibrium; exclusive bus lane; synthetic proportional index

---

1. INTRODUCTION

Choice captivity has long been recognized in the travel choice problems, particularly for the mode choice behavior (Gaudry and Dagenais, 1979; Gaudry, 2015), where some travelers rely on one specific mode of transportation (i.e., captive to one mode), and do not have the freedom to select all travel modes according to social, economic, and physical constraints. Mode captivity has been reported in different cities with significant proportions around the world. McCarthy (1997) reported that more than 48 percent of the American inter-city passengers were captive to the auto mode. Similar results were found for intra-city transport in other cities around the world (Beimborn et al., 2003; Saleh and Al-Atawi, 2015). The transit market observed similar situations, about 70 percent transit riders according to the 1995 Nationwide Personal Transportation Survey in the USA (Polzin et al, 2000) and 51 percent motorized trips in Johannesburg, South Africa (Venter, 2016) were captive to the public transit system.

The captive mode travelers, according to Swait and Ben-Akiva (1986) and Ergün et al. (1999), are less sensitive to changes in the level of service (e.g., travel time) of other modes and have a significant impact on the travel mode market segmentation (Lee and Cunningham, 1996; Krizek and El-Geneidy, 2007). As a result, ignoring mode captivity has the risk of over-estimating model parameters, misrepresenting and misinterpreting transportation policies (Williams and Ortuzar, 1982; Swait and Ben-Akiva, 1987; Van Exel and Rietveld, 2001; Habib and Weiss, 2014), while accounting for captive mode travelers would significantly improve the accuracy of mode share predictions (Srinivasan et al., 2007; Venter, 2016).

In fact, the captive choice behavior has been considered in other dimensions in the combined travel choice framework, such as captive destination choice due to enforced work trips (Chu, 1990, 2011, 2018), captive departure time choice (Chu, 2009) and car ownership decision (Chu, 2016). However, captivity in mode choice, through which the concept of captivity was first introduced into the transportation domain, has seldom been considered in the combined travel choice framework. To fill this gap, this paper considers the captive mode choice behavior in the combined travel choice problem. Specially, we consider the multi-modal network equilibrium (MMNE) problem to investigate the impacts of mode captivity on the mode and route choices.

The following provides a brief review of the research related to the MMNE problems, in terms of consideration of mode captivity, improvements on the mode and route choice models, and applications to motivate the present study and highlight the contributions of this study.

The MMNE model is often adopted to analyze travelers' mode and route choices under congestion (Szeto et al., 2012). More specifically, the MMNE model is particularly suitable for analyzing transportation networks involving multiple travel modes, since it can resolve the inconsistency issue of the 4-step sequential transportation planning approach. Early efforts focused on the modeling of MMNE problems and assumed deterministic route choice and stochastic mode choice, which are captured respectively by the user equilibrium (UE) model

and random utility maximization (RUM) model (Florian, 1977; Florian and Nguyen, 1978; Abdulaal and LeBlanc, 1979; Cantarella, 1997; Boilé and Spasovic, 2000). Based on these early works, later efforts were paid to improve the MMNE model in terms of route and /or mode choice models, and applications.

At the route choice level, the first efforts were paid to overcome the inconsistency between the UE-based route choice and RUM-based mode choice in the above MMNE models, Oppenheim (1995) and Wu and Lam (2003) applied the MNL model for both mode and route choices. Some efforts focused on integrating advanced discrete choice models for capturing travelers' complex route behavior. Meng and Liu (2012) and Wang et al. (2018a) applied respectively, the multinomial probit (MNP) model and the paired combinatorial logit (PCL) model, to capture the correlation among routes.

At the mode choice level, García and Marín (2005) and Yao et al. (2018) adopted the nested logit (NL) model to consider mode similarity; Liu et al. (2018) took the cross nested logit (CNL) model to describe the mode choice with rail-based park-and-ride option. Notably, Kitthamkesorn et al. (2016) adopted respectively the NL model and the CNL model to capture the mode similarity and route overlapping and ensure the in-between consistency in the meantime. Further, Kitthamkesorn and Chen (2017) integrated the nested weibit (NW) mode choice model and the path-size weibit (PSW) route choice model to allow mode-specific and route-specific perception variances consistently.

In terms of applications, these MMNE models were applied for optimal network design problems (Liu et al, 2018; Wang et al., 2015), exclusive bus lane setting and bus operation optimization problems (Yao et al., 2012, 2015, 2018), optimal toll design problems (Meng and Liu, 2012) and transportation strategy evaluation problems (Kitthamkesorn et al., 2016; Kitthamkesorn and Chen, 2017; Li et al., 2015). A summary of research on the multi-modal network equilibrium problems is presented in Table 1.

Table 1. Selected research on the multi-modal network equilibrium models

Improvement perspectives	Reference	Mode captivity	Model	Remark
Initiating efforts	Florian (1977), Florian and Nguyen (1978), Abdulaal and LeBlanc (1979), Cantarella (1997) and Boilé and Spasovic (2000)	No	MNL-UE	Focus on the modeling of the MNL-UE MMNE problem
Improvements on route choice model	Oppenheim (1995)	No	MNL-MNL	Provide an MP formulation for the MNL-MNL MMNE problem
	Wu and Lam (2003)	No	MNL-MNL	Provide a VI formulation for the MNL-MNL MMNE problem
	Meng and Liu (2012)	No	Binary Logit-MNP	Apply the Binary-Logit-MNP MMNE model in the cordon-based toll design problem
	Wang et al. (2018a)	No	MNL-PCL	Develop and apply the MNL-PCL MMNE model for sensitivity-analysis based critical parameter analysis and uncertainty analysis etc.
Improvements on mode choice model	Yao et al. (2012; 2015)	No	MNL-UE	Apply the MNL-UE MMNE model in the optimization of exclusive bus lane (EBL) and bus operation frequency
	Yao et al. (2018)	No	NL-UE	Consider NL-based mode choice among solo driving, bus, and ride-sharing, and apply the NL-UE MMNE model in the optimization of EBL settings (whether to share or not) and bus operation frequencies
	García and Marín (2005)	No	NL-UE	Consider NL-based mode and transfer choice
	Liu et al. (2018)	No	CNL-UE	Consider CNL-based mode and transfer choice, and apply the CNL-UE MMNE model in the rail-based park and ride design
Improvements on both mode and route choice models	Kitthamkesorn et al. (2016)	No	NL-CNL	Capture both the modal and route similarity by respectively the NL and CNL models, apply the NL-CNL MMNE model in the evaluation of different “go-green” promotion policies
	Kitthamkesorn and Chen (2017)	No	NW-PSW	Consider cost-based perception variances and modal and route similarity, apply the NW-PSW MMNE model in the evaluation of go-green versus go-grey mode promotion policies

One limitation of the above MMNE models is that they all assume full availability of all travel modes for every traveler. However, as aforementioned, some travelers are captive to one travel mode for most daily trips due to social, economic, and physical issues. Few studies consider mode captivity in the combined travel choice problems, only one paper (to the best of our knowledge) focuses on algorithm development for solving an MMNE problem with considering captive mode traveler and route overlapping (Ryu et al., 2018). In this paper, we consider the captive mode travelers in the MMNE problem by adopting the dogit model (Gaudry and Dagenais, 1979) to consider the captive mode choice behavior, and the path-size logit (PSL, Ben-Akiva and Bierlaire, 1999) model to represent the route choice behavior with route overlapping consideration. Specifically, a mathematical programming (MP) formulation is proposed for the dogit-PSL MMNE model, together with proofs of equivalence and solution uniqueness. Numerical examples are carried out to investigate the impacts of mode captivity and route overlapping on equilibrium network states and performances.

Also, in viewing that public transportation is playing a critical role in the multi-modal urban transportation system, particularly for some densely populated Asian cities like Hong Kong, public transit takes up most of the daily travel demand (Transport Department, 2018), it would be problematic to ignore public transportation or the captive mode travelers. Hence, it is interesting and necessary to investigate the impacts of mode captivity (structure) on the optimization of public transportation strategies. An application of the dogit-PSL MMNE model on evaluating the exclusive bus lane (EBL) expansion plans is carried out under different scenarios. A consistent synthetic proportional index is defined to quantify the relative improvement of network total travel time (TTT) and emission after the expansion operation. Numerical results show that considering mode captivity in the MMNE problem produces substantially different estimations of the impacts of EBL expansion policies, and significantly increase the chances (up to 50 percent of odds) of making different EBL line expansion decisions in the given settings.

The paper contributes to the literature in two aspects:

(1) We consider captive mode travelers in a multi-modal network equilibrium (MMNE) model, and formulate it as an equivalent mathematical programming problem with a unique solution; the MMNE model is applied to evaluate the EBL expansion choices, in which a weighted synthetic index is proposed to quantify the proportional improvements of the two-dimensional network performance indices, which ensures consistent dominance relationship with the collective network performance indices but avoid the dimensional effect.

(2) We apply the MMNE model with captive mode travelers to a real-size multi-modal network with 107,434 O-D pairs and a total of 2.9 million daily trips. The numerical example demonstrates the applicability of the proposed model, and also the impacts of captive mode travelers on the combined mode and route choices.

The study proceeds as follows. Section 2 provides a brief review of the dogit and PSL models, follows with an equivalent MP formulation for the dogit-PSL MMNE problem in Section 3. Sections 4 provides a path-based solution algorithm for solving the MMNE problem. In Section 5, three numerical examples are provided to examine the impacts of captive mode travelers and route overlapping on network equilibrium, to show an application on evaluating exclusive bus lane expansion plans and the applicability of the algorithm for the real-size network. The paper concludes with discussions in Section 6.

2. METHODOLOGICAL BACKGROUND

This section provides background on the dogit model and the PSL model, which are adopted for accommodating the captivity effect in the modal split problem and the route overlapping effect in the traffic assignment problem, respectively.

2.1. Notation

The following notation is used in the model formulation:

Indices

A	Set of all links
M	Set of all modes
IJ	Set of origin-destination (O-D) pairs
A_{ij}^{mr}	Set of links on route $r \in R_{ij}^{m}$ in mode $m \in M_{ij}$ between O-D pair $ij \in IJ$
M_{ij}	Set of modes between O-D pair $ij \in IJ$
R_{ij}^{m}	Set of routes in mode $m \in M_{ij}$ between O-D pair $ij \in IJ$

Parameters

η_{ij}^{m}	Captivity parameter for mode $m \in M_{ij}$ between O-D pair $ij \in IJ$
$\hat{\eta}_{ij}^{m}$	Scaled captivity parameter for mode $m \in M_{ij}$ between O-D pair $ij \in IJ$ defined by $\hat{\eta}_{ij}^{m} = \zeta \eta_{ij}^{m}, \forall m, ij$
ζ	Scale parameter for the system mode captivity level
q_{ij}	Travel demand between O-D pair $ij \in IJ$
C^{ma}	The capacity of link $a \in A$ in mode $m \in M$
l^{a}	Length of link $a \in A$
L_{ij}^{mr}	Length of route $r \in R_{ij}$ between O-D pair $ij \in IJ$
α, β	Parameters of the Bureau of Public Roads link travel time function
δ_{ij}^{mra}	Path-link-mode incidence indicator for link $a \in A_{ij}^{mr}$ and route $r \in R_{ij}^{m}$ in mode $m \in M_{ij}$ between O-D pair $ij \in IJ$

ϖ_{ij}^{mr} The path-size factor for route $r \in R_{ij}^{m}$ in mode $m \in M_{ij}$ between O-D pair $ij \in IJ$

Ψ_{ij}^{m} The exogenous utility of mode $m \in M_{ij}$ between O-D pair $ij \in IJ$

θ_{ij}^{m} Dispersion parameter for route choice in mode $m \in M_{ij}$ between O-D pair $ij \in IJ$

θ_{ij}^{um} Dispersion parameter of route choice in mode $m \in M_{ij}$ under nest u between O-D pair $ij \in IJ$

γ_{ij} Scale parameter for mode choice between O-D pair $ij \in IJ$

ϕ_{ij}^{u} Scale parameter for mode nest u between O-D pair $ij \in IJ$ in the nested logit modal split model

ϑ_{TTT} Dimensionless weight parameter of network TTT

Γ, τ Parameters for the self-regulated averaging line search scheme

Intermediate Variables

P_{ij}^{m} Choice probability of mode $m \in M_{ij}$ between O-D pair $ij \in IJ$

P_{ij}^{mr} Choice probability of route $r \in R_{ij}^{m}$ in mode $m \in M_{ij}$ between O-D pair $ij \in IJ$

h^{ma} Travel cost (time) of link $a \in A$ in mode $m \in M$

U_{ij}^{m} Deterministic (observable) utility of mode $m \in M_{ij}$ between O-D pair $ij \in IJ$

V_{ij}^{m} Expected perceived disutility of mode $m \in M_{ij}$ between O-D pair $ij \in IJ$

w_{ij}^{mr} Expected travel cost on route $r \in R_{ij}^{m}$ in mode $m \in M_{ij}$ between O-D pair $ij \in IJ$

λ_{ij} Dual variable for the demand conservation constraint between O-D pair $ij \in IJ$

φ_{ij}^{m} Dual variable for the flow conservation constraint in mode $m \in M_{ij}$ between O-D pair $ij \in IJ$

TTT, E Network total travel time and total emission

$SI_{\mathrm{model}}^{\mathrm{AEP}i}$ Synthetic impact of taking an alternative expansion plan AEP*i* in model 'model'

Decision Variables

q_{ij}^{m} Travel demand of mode $m \in M_{ij}$ between O-D pair $ij \in IJ$

f_{ij}^{mr} Traffic flow on route $r \in R_{ij}^{m}$ in mode $m \in M_{ij}$ between O-D pair $ij \in IJ$

v^{ma} Traffic flow on link $a \in A$ in mode $m \in M$

2.2. Dogit Model

Gaudry and Dagenais (1979) originally proposed the dogit model to permit flexibility in handling choice among the captive choice sets where each consists of a single-choice alternative and the full choice set which contains all the choice alternatives under consideration. The dogit mode choice probability can be expressed as

$$P_{ij}^{m}=\frac{\exp\left(\gamma_{ij}U_{ij}^{m}\right)+\eta_{ij}^{m}\sum_{n\in M_{ij}}\exp\left(\gamma_{ij}U_{ij}^{n}\right)}{\left(1+\sum_{n\in M_{ij}}\eta_{ij}^{n}\right)\sum_{n\in M_{ij}}\exp\left(\gamma_{ij}U_{ij}^{n}\right)},\quad \forall m\in M, ij\in IJ \tag{1}$$

where U_{ij}^{m} is the deterministic utility of mode m between origin and destination (O-D) pair ij, γ_{ij} is the scale parameter for mode choice and $\eta_{ij}^{m}\geq 0$ is the captivity parameter of mode m between O-D pair ij. Rearranging Eq. (1) yields

$$P_{ij}^{m}=\underbrace{\frac{\eta_{ij}^{m}}{1+\sum_{n\in M_{ij}}\eta_{ij}^{n}}(\cdot 1)}_{\text{Captive share}}+\underbrace{\frac{1}{1+\sum_{n\in M_{ij}}\eta_{ij}^{n}}}_{\text{Choice share}}\underbrace{\frac{\exp(\gamma_{ij}U_{ij}^{m})}{\sum_{n\in M_{ij}}\exp(\gamma_{ij}U_{ij}^{n})}}_{\text{Logit Assignment}},\quad \forall m\in M_{ij}, ij\in IJ. \tag{2}$$

The first term on the right-hand side of Eq. (2) denotes the share of travelers who are captive to mode m, and the second term represents the share of choice travelers choosing mode m, which is the product of the proportion of all choice travelers and the multinomial logit (MNL) probability of choosing mode m.

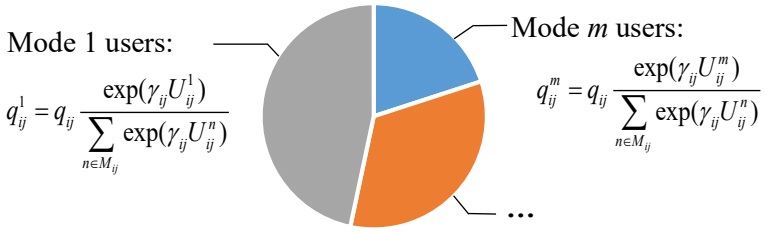

(1) MNL modal split

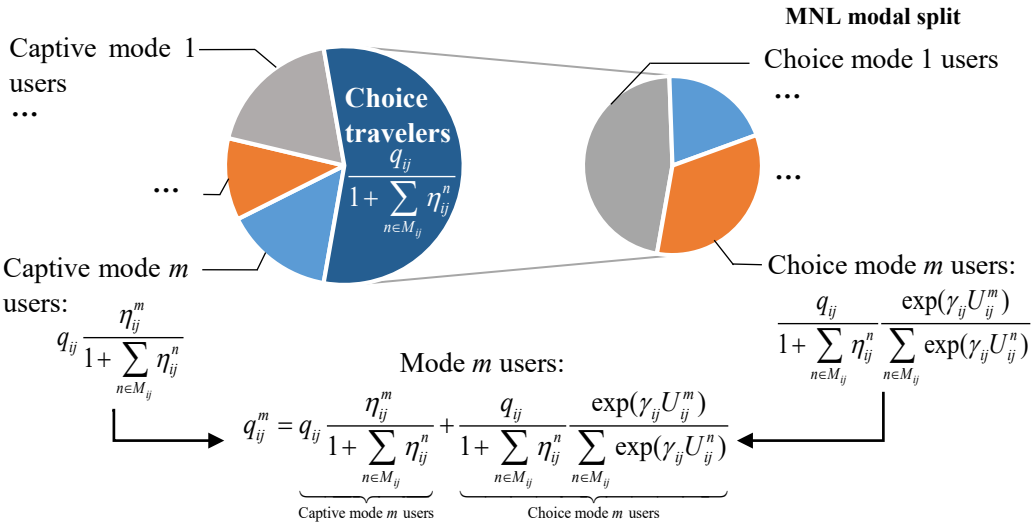

(2) Dogit modal split

Fig. 1. The MNL and dogit modal splits

Fig. 1 uses two pie charts to compare the MNL and dogit modal split processes. In the MNL model, travelers have access to all travel modes and split following the MNL model. While in the dogit model, trip demand of a mode (e.g., m) consists of two parts, the travelers who are

captive to mode m determined by the mode captivity parameters (i.e., $q_{ij}\eta_{ij}^{m} \Big/ (1+\sum_{n\in M_{ij}} \eta_{ij}^{n})$), and the choice travelers who select mode m following the MNL modal splits (i.e., $\frac{q_{ij}}{1+\sum_{n\in M_{ij}} \eta_{ij}^{n}} \frac{\exp(\gamma_{ij} U_{ij}^{m})}{\sum_{n\in M_{ij}} \exp(\gamma_{ij} U_{ij}^{n})}$).

Note that, there are different ways for the discrete choice modeling of captive mode choice behavior, such as adding an implicit availability indicator to the utility function (Cascetta and Papola, 2001), parameterizing mode captivity as a function of random constraints (Swait et al., 1987), or modeling the probabilistic availability of a choice with a threshold-based cut-off function (Martínez et al., 2009). However, most of these discrete choice models do not have a close-form choice probability and are hard to be incorporated in the entropy-based mathematical programming network equilibrium models. Therefore, we choose the dogit model to describe the captive mode choice behavior in the joint mode-route choice problem.

2.2.1. *An illustrative numerical example*

In this section, we present an illustrative numerical example to show the dogit modal split process and also its sensitivity with respect to (w.r.t.) mode captivity parameter and mode travel time, by comparing to those of the MNL model. In the one origin-destination (O-D) network, two travel modes are considered, i.e., auto and bus. The total travel demand is set to 1, and the auto and bus travel times are set to 8.150 and 12.205 time units, respectively. The deterministic modal utility is defined as the negative of mode travel time. The O-D scale parameter is set to 0.1, and the auto and bus captivity parameters are set respectively to 0.3 and 0.7, which means half of the total trip demand are captive to one travel mode (i.e., $\frac{0.3+0.7}{1+0.3+0.7}=0.5$).

Fig. 2 shows the dogit modal split process. Compared to the MNL modal split as presented in Fig. 2-1, the dogit model (Fig. 2-2) groups the total travel demand into three classes for the two-mode case, i.e., the captive auto travelers, captive bus travelers, and choice travelers. The trip demand for each mode consists of two parts, i.e., the captive trip demand and the choice ones following the MNL modal split. In the current case, the auto and bus modes have respectively 0.15 and 0.35 captive trip demand, leaving only 50 percent of the total trip demand who can freely choose between auto and bus. As a consequence, the total auto trip demand is 0.15+0.5*0.6=0.45, significantly smaller than the MNL modal split prediction (i.e., 0.6). Fig. 2 shows that, considering the captive mode travelers may produce different modal split predictions.

In Fig. 3, we examine the sensitivity of dogit modal split w.r.t. mode captivity parameter. We vary the auto captivity parameter from 0 to 1 at an interval of 0.1, while keeping the sum of the two mode captivity parameters being equal to 1 at the same time. As Fig. 3 depicted, the MNL modal split shows no response to the change of auto captivity parameter η_{ij}^{Auto}. At the same time, the total dogit auto flow increases along with η_{ij}^{Auto}, among which the choice auto demand

is unaffected, while the captive auto demand increases w.r.t. η_{ij}^{Auto}. Hence, when the total size of captive mode travelers is fixed, increasing the captivity parameter of one mode would increase the total travel demand of that mode by adding more captive mode travelers.

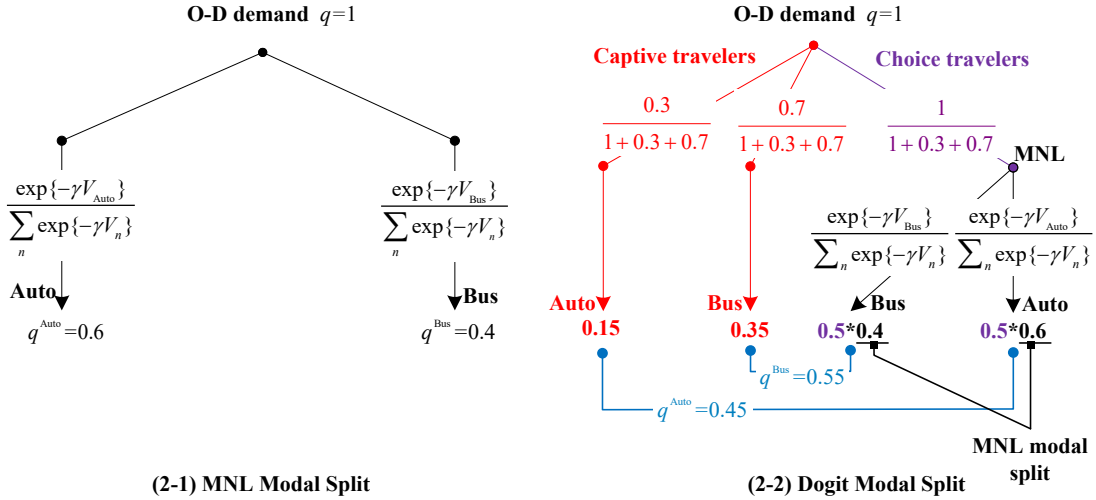

(2-1) MNL Modal Split (2-2) Dogit Modal Split

Note: 1. O-D dispersion parameter γ=0.1;
2. Auto and bus mode travel times V_{mode} are set to 8.150 and 12.205 time units, respectively;
3. Auto and bus captivity parameters are respectively set to 0.3 and 0.7.

Fig. 2. Comparison of the MNL and dogit modal splits

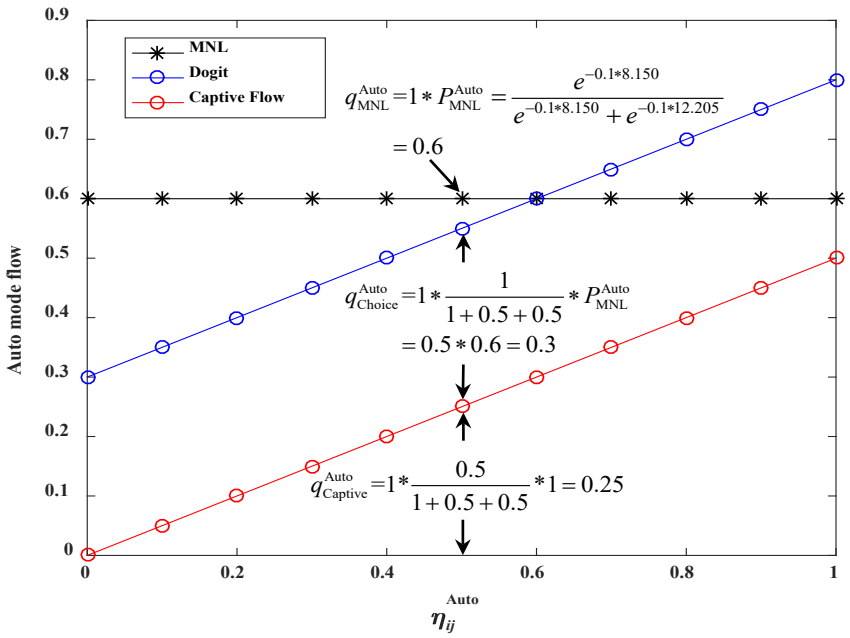

Fig. 3. Changes in auto mode flow w.r.t. captivity parameter

In Fig. 4, we further examine the sensitivity of dogit modal split w.r.t. mode travel time. We vary the auto travel time from 3.150 to 13.150 at an interval of 1.0 and keep the bus travel time unchanged. As the auto travel time increases, the MNL auto flow decreases from 0.7 to less than 0.5, so does the dogit auto flow. However, the latter decreases slower than the MNL auto flow from 0.5 to about 0.4, among which the captive auto flow shows no response to the changes in auto travel time. Therefore, we may conclude that increasing the travel time of one mode would decrease the dogit travel demand of that mode, however, less significantly than the MNL

prediction. To put it in another way, the captive mode travelers would bring down the sensitivity of dogit modal split w.r.t. mode travel time changes.

Note that we use presumed input parameters to demonstrate the impacts of mode captivity and mode travel costs on the modal splits. When examining and comparing the validities of different models, care must be taken, a fair comparison of model validities should be conducted based on the same given household survey data, and the comparison should include both parameter estimation and prediction.

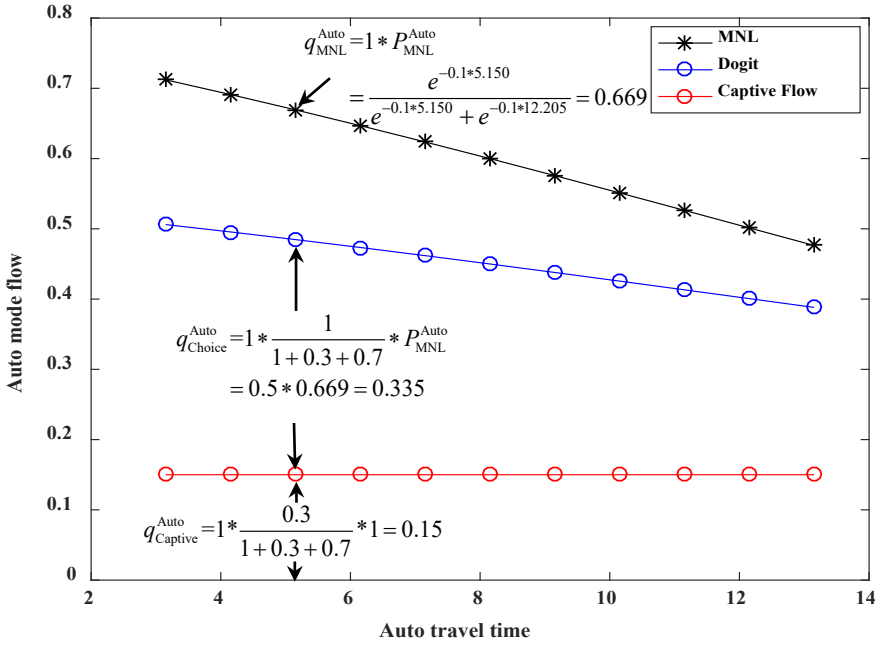

Fig. 4. Changes in auto mode flow w.r.t. auto travel time

2.3. PATH-SIZE LOGIT MODEL

The path-size logit model was developed by Ben-Akiva and Bierlaire (1999) to handle the route overlapping problem. The conditional PSL route choice probability in mode *m* is expressed as

$$P_{ij}^{r|m} = \frac{\varpi_{ij}^{mr} \exp(-\theta_{ij}^{m} w_{ij}^{mr})}{\sum_{k \in R_{ij}} \varpi_{ij}^{mk} \exp(-\theta_{ij}^{m} w_{ij}^{mk})}, \quad \forall r \in R_{ij}^{m}, m \in M_{ij}, ij \in IJ, \tag{3}$$

where w_{ij}^{mr} is the travel cost (time) on route *r* in mode *m* between the O-D pair *ij*, θ_{ij}^{m} is the dispersion parameter, and $\varpi_{ij}^{r} \in (0,1]$ is the path-size factor defined by

$$\varpi_{ij}^{mr} = \sum_{a \in A_{ij}^{mr}} \frac{l^{a}}{L_{ij}^{mr}} \frac{1}{\sum_{k \in R_{ij}^{m}} \delta_{ij}^{mka}}, \quad \forall r \in R_{ij}^{m}, m \in M_{ij}, ij \in IJ, \tag{4}$$

with l^{a} and L_{ij}^{mr} are respectively the lengths of link *a* and route *r* in mode *m* between O-D pair *ij*, A_{ij}^{mr} is the set of links on route *r* in mode *m* between O-D pair *ij*, and $\delta_{ij}^{mra} = \{0,1\}$ is

a binary path-link-mode incidence indicator. The path-size factor ϖ_{ij}^{mr} measures the degree of route *r* being shared (overlapped) by other routes in mode *m* between O-D pair *ij*. It is defined as an average of the inverse of the number of each link on route *r* being used by other routes in the same mode between the same O-D pair, i.e. $1\Big/\sum_{k\in R_{ij}^{m}}\delta_{ij}^{mka}$ ($\forall a\in A_{ij}^{mr}$), weighted by the ratio of the length of each link over that of route *r* in mode *m* between O-D pair *ij*, i.e. $l_{ij}^{mra}\Big/L_{ij}^{mr}$ ($\forall a\in A_{ij}^{mr}$). Routes with a heavy overlap with others have small values of ϖ_{ij}^{mr}. The following uses a loop-hole network to illustrate the effect of route overlapping for the sake of completeness.

The loop-hole network is presented in Fig. 5, in which route 1 uses link 2 and shares link 1 with route 2, route 3 uses a separate link 4, the basic settings of the loop-hole network is presented in Table 2. The link free-flow travel speed is set to 1 km/minute; then we have the link free-flow travel time (FFTT) is equal to the link length. We vary the length of link 1 from 18 to 0 at an interval of -1 and investigate the route choice probability as a function of route path-size factor and link FFTTs. The route choice dispersion parameter is set to 1.2.

Route choice probabilities in the MNL and PSL models are shown in Fig. 6. In the MNL model, all three routes have the same route FFTT and accordingly, the equal route choice probability. Comparatively, by considering route overlapping in the PSL model, the overlapped routes (i.e., routes 1 and 2) have smaller choice probabilities than those in the MNL model. As the path size factor of route 1 increases (i.e., being less overlapped with other routes as a result of smaller *x*), we have larger choice probabilities for route 1 in the meantime.

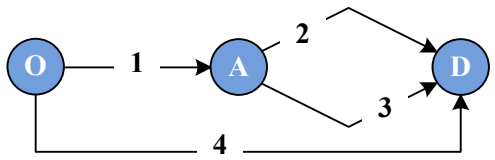

Fig. 5. The loop-hole network

Table 2. Settings of the loop-hole network

Aspects	**Auto**			
Link	1	2	3	4
Length (kilometer)	*x*	18-*x*	18-*x*	18
FFTT (minute)	*x*	18-*x*	18-*x*	18

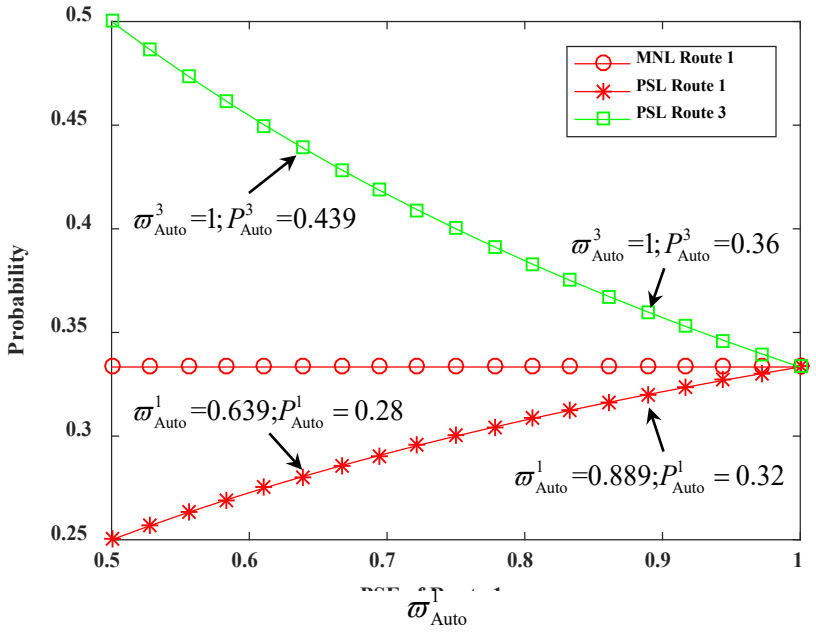

Fig. 6. Route choice probability under different PSF values

2.4. Joint Choice Probability

Based on the dogit mode choice probability in Eq. (1) and the conditional PSL route choice probability in Eq. (3), we have the joint mode-route choice probability as follows:

$$P_{ij}^{mr} = P_{ij}^{m} \cdot P_{ij}^{r|m} = \frac{\exp\left(\gamma_{ij} U_{ij}^{m}\right) + \eta_{ij}^{m} \sum_{n \in M_{ij}} \exp\left(\gamma_{ij} U_{ij}^{n}\right)}{\left(1 + \sum_{n \in M_{ij}} \eta_{ij}^{n}\right) \sum_{n \in M_{ij}} \exp\left(\gamma_{ij} U_{ij}^{n}\right)} \cdot \frac{\varpi_{ij}^{mr} \exp(-\theta_{ij}^{m} w_{ij}^{mr})}{\sum_{k \in R_{ij}^{m}} \varpi_{ij}^{mk} \exp(-\theta_{ij}^{m} w_{ij}^{mk})} . \tag{5}$$

The joint mode-route choices are determined simultaneously. In the mode choices, the captive mode travelers constitute a constant share for each mode, while the choice travelers split across different modes according to the MNL probability, as a function of deterministic modal utility U_{ij}^{m} and the mode choice scale parameter γ_{ij}. Given the mode choice between each O-D pair, travelers determine their mode-specific route choice probabilities according to the PSL probability in Eq. (3), as a function of mode-specific route travel cost w_{ij}^{mr}, the path-size factor ϖ_{ij}^{mr} in Eq. (4) and the route choice dispersion parameter θ_{ij}^{m}. The conditional route choice connects to the marginal mode choice by affecting the deterministic modal utility $U_{ij}^{m} = \Psi_{ij}^{m} - V_{ij}^{m}$, particularly the inclusive disutility part, i.e., the expected modal perceived travel cost or the log-sum term $V_{ij}^{m} = \frac{-1}{\theta_{ij}^{m}} \log \sum_{k \in R_{ij}} \varpi_{ij}^{mk} \exp(-\theta_{ij}^{m} w_{ij}^{mk})$, which then affects the marginal mode choice probabilities. In the deterministic modal utility U_{ij}^{m}, Ψ_{ij}^{m} is the

exogenous utility of mode $m \in M_{ij}$ between O-D pair $ij \in IJ$ to account for the attributes which are not considered in V_{ij}^{m} or w_{ij}^{mk}, e.g., fare, convenience and comfort, etc.

Remark. In the joint dogit-PSL model, two types of input parameters need to be estimated by fitting the model (or other models) to some dataset, i.e., the captivity parameter for each mode and the scale or dispersion parameters for mode and route choices. We may generally have two ways to estimate these two types of input parameters. In the first approach, we may use a two-stage method to firstly estimate the mode captivity and scale parameters and then evaluate the dispersion parameter for route choices. In this case, the mode captivity consists of both captivity by choice (i.e., latent/implicit mode captivity) and captivity by force (Jacques et al., 2013). We could treat the mode captivity parameters (Swait and Ben-Akiva, 1986, 1987; Beimborn et al., 2003; Habib and Weiss, 2014) and the scale parameters for mode choice (Habib and Weiss, 2014) as a function of independent variables, such as private vehicle availability, transit connectivity, walk/bicycle access to a transit station, occupation, number of vehicles owned, age, trip length, trip purpose etc. Hence in the first stage, we may estimate the mode captivity and scale parameters independently. In the second stage, we take the mode captivity parameters and travelers' mode-route choice data as input and estimate the dispersion parameters for the route choices. The benefits of estimating the mode captivity parameters independently are that we can parameterize these parameters and consider complex behavioral or econometric factors that bear managerial meanings. The cost is that we need more data (both individual econometric data and travel diary data or mode-route choice data) to conduct the two-stage estimations, run the risk of obtaining inconsistent or unreasonable results.

In the second approach, we may jointly estimate the two types of parameters based on the combined mode-route choice data. The mode captivity parameters are treated the same as other parameters to estimate (McCarthy, 1997; Gaudry and Wills, 1979; Gaudry, 1980, 1981). The methods of maximum likelihood estimate or ordinary least square can be applied for these estimations. For the evaluation of combined travel choice model with captive behaviors, Dr. Chu has conducted a series of modeling and calibration studies, including captive destination choice due to compulsory work trips (Chu, 1990, 2011, 2018), captive departure time choice (Chu, 2009) and car ownership decisions (Chu, 2016), in the combined travel choice framework. The second approach assures better consistency between the mode and route choice predictions and has less input data requirement; however, at the loss of behavioral richness.

3. MATHEMATICAL PROGRAMMING FORMULATIONS

In this section, an equivalent MP formulation for the dogit-PSL MMNE model is developed. Before presenting the MMNE formulation, three assumptions are made as follows.

Assumption 1. The mode networks are independent from each other. Thus, the travel time of mode *m* on link *a* is a function of the mode flow v^{ma} on link *a* only.

Assumption 2. The link-mode travel time is a monotonically increasing function of its own mode flow.

Assumption 3. The path-size factor is a function of the free-flow travel cost.

3.1. DOGIT-PSL MULTI-MODAL NETWORK EQUILIBRIUM MODEL

Based on the dogit mode choice model (1) - (2) and the PSL traffic assignment model (3)- (4), an equivalent MP formulation for the dogit-PSL MMNE model is presented as follows:

$$\begin{aligned}\min Z &= Z_1 + Z_2 + Z_3 + Z_4 + Z_5 + Z_6 \\ &= \sum_{m\in M_{ij}}\sum_{a\in A}\int_0^{v^{ma}=\sum_{ij\in IJ}\sum_{r\in R_{ijm}} f_{ij}^{mr}\delta_{ij}^{mra}} h^{ma}(\omega)\,d\omega + \sum_{ij\in IJ}\sum_{m\in M_{ij}}\frac{1}{\theta_{ij}^{m}}\sum_{r\in R_{ij}} f_{ij}^{mr}\left(\ln f_{ij}^{mr}-1\right) \\ &\quad -\sum_{ij\in IJ}\sum_{m\in M_{ij}}\frac{1}{\theta_{ij}^{m}}\sum_{r\in R_{ij}^{m}} f_{ij}^{mr}\ln\varpi_{ij}^{mr} + \sum_{ij\in IJ}\frac{1}{\gamma_{ij}}\sum_{m\in M_{ij}}\left(q_{ij}^{m}-\frac{\eta_{ij}^{m}}{1+\sum_{m\in M_{ij}}\eta_{ij}^{n}}q_{ij}\right) \\ &\quad *\left[\ln\left(q_{ij}^{m}-\frac{\eta_{ij}^{m}}{1+\sum_{m\in M_{ij}}\eta_{ij}^{n}}q_{ij}\right)-1\right] - \sum_{ij\in IJ}\sum_{m\in M_{ij}}\frac{1}{\theta_{ij}^{m}}q_{ij}^{m}\left(\ln q_{ij}^{m}-1\right) - \sum_{ij\in IJ}\sum_{m\in M_{ij}} q_{ij}^{m}\Psi_{ij}^{m}.\end{aligned} \tag{6.1}$$

s.t.

$$\sum_{m\in M_{ij}} q_{ij}^{m} = q_{ij}\,,\quad \forall ij\in IJ\,, \tag{6.2}$$

$$\sum_{r\in R_{ij}^{m}} f_{ij}^{mr} = q_{ij}^{m}\,,\quad \forall m\in M_{ij}, ij\in IJ\,, \tag{6.3}$$

$$q_{ij}^{m}\ge 0\,,\quad \forall m\in M_{ij}, ij\in IJ\,, \tag{6.4}$$

$$f_{ij}^{mr}\ge 0\,,\quad \forall r\in R_{ij}^{m}, m\in M_{ij}, ij\in IJ\,, \tag{6.5}$$

where f_{ij}^{mr} is the flow on route *r* in mode *m* between O-D pair *ij*, v^{ma} is the flow on link *a* in mode *m*, h^{ma} is the travel cost on link *a* in mode *m*, and Ψ_{ij}^{m} is the exogenous utility of mode *m* between O-D pair *ij*. In Eq. (6.1), Z_1 is the well-known Beckmann transformation, Z_2 captures the stochastic perception error in route choices, Z_3 uses a path-size factor to penalize the overlapping among routes, Z_4 and Z_5 are entropy terms related to respectively the mode choice of choice travelers and that of all travelers to account for the captive mode travelers in the mode split problem. In fact, we omit the constant entropy term for the mode choice of captive mode travelers since their mode choices are fixed. Z_6 handles the exogenous mode attractiveness. Eqs. (6.2) and (6.3) are flow conservation constraints and Eqs. (6.4) and (6.5) are non-negative

constraints. The MP formulation (6.1)- (6.5) has some qualitative properties, as stated in the following two propositions:

Proposition 1. *The MP formulation in Eqs. (6.1)- (6.5) gives the route choice solution of the PSL model and the mode choice solution of the dogit model.*

Proof. The Lagrangian of the objective function Eq. (6.1) w.r.t. the flow conservation constraints Eqs. (6.2)- (6.3) is defined by

$$L = Z + \sum_{ij} \lambda_{ij} \left(\sum_{m} q_{ij}^{m} - q_{ij} \right) + \sum_{ij} \sum_{m} \varphi_{ij}^{m} \left(\sum_{r} f_{ij}^{mr} - q_{ij}^{m} \right) \tag{7}$$

where λ_{ij} and φ_{ij}^{m} denote the dual variables for the flow conservation constraints in Eq. (6.2) and Eq. (6.3), respectively.

(1) Take the partial derivative of the Lagrangian L w.r.t. the mode-route flows f_{ij}^{mr}, we have

$$\frac{\partial L}{\partial f_{ij}^{mr}} = 0 \Rightarrow w_{ij}^{mr} + \frac{1}{\theta_{ij}^{m}} \ln f_{ij}^{mr} - \frac{1}{\theta_{ij}^{m}} \ln \varpi_{ij}^{mr} + \varphi_{ij}^{m} = 0 \tag{8}$$

$$\Rightarrow f_{ij}^{mr} = \exp\{-\theta_{ij}^{m} \varphi_{ij}^{m}\} \varpi_{ij}^{mr} \exp\{-\theta_{ij}^{m} w_{ij}^{mr}\} . \tag{9}$$

Then, we have the O-D mode flow by summing Eq. (9) over r

$$q_{ij}^{m} = \sum_{r \in R_{ij}^{m}} f_{ij}^{mr} = \exp\{-\theta_{ij}^{m} \varphi_{ij}^{m}\} \sum_{r \in R_{ij}^{m}} \varpi_{ij}^{mr} \exp\{-\theta_{ij}^{m} w_{ij}^{mr}\} . \tag{10}$$

Dividing Eq. (9) by Eq. (10) gives the mode-route choice probability $P_{ij}^{(r|m)}$:

$$P_{ij}^{(r|m)} = \frac{f_{ij}^{mr}}{q_{ij}^{m}} = \frac{\exp\{-\theta_{ij}^{m} \varphi_{ij}^{m}\} \varpi_{ij}^{mr} \exp\{-\theta_{ij}^{m} w_{ij}^{mr}\}}{\exp\{-\theta_{ij}^{m} \varphi_{ij}^{m}\} \sum_{r} \varpi_{ij}^{mr} \exp\{-\theta_{ij}^{m} w_{ij}^{mr}\}} = \frac{\varpi_{ij}^{mr} \exp\{-\theta_{ij}^{m} w_{ij}^{mr}\}}{\sum_{k \in R_{ij}} \varpi_{ij}^{mk} \exp\left(-\theta_{ij}^{m} w_{ij}^{mk}\right)} . \tag{11}$$

(2) In a similar way, we get the partial derivative of Lagrangian L w.r.t. q_{ij}^{m}

$$\frac{\partial L}{\partial q_{ij}^{m}} = 0 \Rightarrow \frac{1}{\gamma_{ij}} \ln \left(q_{ij}^{m} - \frac{\eta_{ij}^{m} q_{ij}}{1 + \sum_{n \in M_{ij}} \eta_{ij}^{n}} \right) + \frac{1}{\gamma_{ij}} - \frac{1}{\theta_{ij}^{m}} \ln q_{ij}^{m} + \lambda_{ij} - \varphi_{ij}^{m} - \Psi_{ij}^{m} = 0 . \tag{12}$$

Rearranging Eq. (10) gives

$$-\left(1 / \theta_{ij}^{m} \cdot \ln q_{ij}^{m} + \varphi_{ij}^{m}\right) = -1 / \theta_{ij}^{m} \cdot \ln \sum_{r \in R_{ij}^{m}} \exp\{-\theta_{ij}^{m} w_{ij}^{mr}\} . \tag{13}$$

Let $V_{ij}^{m} = -1 / \theta_{ij}^{m} \cdot \ln \sum_{r \in R_{ij}^{m}} \exp\{-\theta_{ij}^{m} w_{ij}^{mr}\}$ be the expected perceived mode travel cost between O-D pair ij, plug V_{ij}^{m} into Eq. (11) and resort gives

$$q_{ij}^{m} - \frac{\eta_{ij}^{m} q_{ij}}{1 + \sum_{n \in M_{ij}} \eta_{ij}^{n}} = \frac{\exp\left[\gamma_{ij} (\Psi_{ij}^{m} - V_{ij}^{m})\right]}{\exp(\gamma_{ij} \lambda_{ij} + 1)} . \tag{14}$$

Dividing Eq. (14) by its sum over $m \in M_{ij}$ gives the dogit mode choice probability

$$P_{ij}^{m}=\frac{q_{ij}^{m}}{q_{ij}}=\frac{\eta_{ij}^{m}}{1+\sum_{n\in M_{ij}}\eta_{ij}^{n}}+\frac{1}{1+\sum_{n\in M_{ij}}\eta_{ij}^{n}}\frac{\exp\left[\gamma_{ij}(\Psi_{ij}^{m}-V_{ij}^{m})\right]}{\sum_{m\in M_{ij}}\exp\left[\gamma_{ij}(\Psi_{ij}^{m}-V_{ij}^{m})\right]}. \tag{15}$$

This completes the proof. □

Proposition 2. *The dogit-PSL MMNE model yields a unique solution.*

Proof. For the proof of Proposition 2, we need to prove the convexity of the objective function in Eq. (6.1) w.r.t. mode-route flow variables and the convexity of the feasible region. For the latter, it is easy to have the convexity of the feasible region under the linear equality constraints in Eqs. (6.2) and (6.3); the nonnegative constraints Eqs. (6.4) and (6.5) will not affect the convexity of the feasible region. For the objective function, taking the Hessian of $Z_1+Z_2+Z_3$ in Eq. (6.1) w.r.t. the mode-route flow variables gives

$$\frac{\partial^2\left(Z_1+Z_2+Z_3\right)}{\partial f_{ij}^{mr}\partial f_{ij}^{ns}}=\begin{cases}\sum_{a\in A}dh_{ma}/dv_{ma}\cdot\delta_{ij}^{mra}+1/\theta_{ij}^{m}\cdot f_{ij}^{mr}>0;\ m=n,r=s\\ 0\qquad\qquad\qquad;otherwise\end{cases}, \tag{16}$$

which implies the positive definite matrix from Assumptions 1 and 2. The Hessian matrix of the $Z_4+Z_5+Z_6$ w.r.t. the modal demand variables can be expressed as

$$\frac{\partial^2\left(Z_4+Z_5+Z_6\right)}{\partial q_{ij}^{m}\partial q_{ij}^{n}}=\begin{cases}\frac{1}{\gamma_{ij}}\cdot\frac{1}{q_{ij}^{m}-\frac{\eta_{ij}^{m}}{1+\sum_{l\in M_{ij}}\eta_{ij}^{l}}q_{ij}}-\frac{1}{\theta_{ij}^{m}}\cdot\frac{1}{q_{ij}^{m}}>0;m=n\\ 0\qquad\qquad;\text{otherwise}\end{cases}. \tag{17}$$

Setting $\gamma_{ij}<\theta_{ij}^{m}$ implies the positive definite matrix. Thus, the dogit-PSL MMNE model has a unique solution. This completes the proof. □

4. SOLUTION ALGORITHM

In this section, we provide a path-based partial linearization algorithm (e.g., Yang et al., 2013) combined with a self-regulated averaging (SRA) line search strategy (Liu et al., 2009) for solving the dogit-PSL MMNE problem. The partial linearization method belongs to the descent direction algorithm for solving continuous optimization problems (Patriksson, 1994). It applies the dogit probability to determine the auxiliary mode flow and uses the PSL probability to determine the conditional route choice probabilities. The procedure of the partial linearization algorithm is presented as follows:

Step 0. Initialization. Initialize the route-mode flow pattern $f(0)=(f_{ij}^{mr})_{\sum_{ij,m}|R_{ij}^{m}|}$ ($|R_{ij}^{m}|$ is the cardinality of route set R_{ij}^{m}), the link-mode flow $v^{ma}=0(\forall a,m)$, the mode captivity parameter between each O-D pair $\eta_{ij}^{m}(\forall m,ij)$, the route choice and mode choice dispersion parameters $\theta_{ij}^{m}(\theta_{ij}^{um},\forall m,ij)$ and $\gamma_{ij}(\forall ij)$ and the convergence criterion ε, set *iter*=0;

Step 1. Update mode-specific link and route travel times $h^{ma}(\forall a,m)$ and $w_{ij}^{mr}(\forall r,m,ij)$, compute generalized mode travel cost between each O-D pair $V_{ij}^{m}(\forall m,ij)$;

Step 2. Determine the search direction. Compute the auxiliary flow pattern $\hat{f}(iter)=(f_{ij}^{mr})_{\sum_{ij,m}|R_{ij}^{m}|}$, define the search direction as the difference between the current flow pattern and the auxiliary flow pattern $\bar{f}(iter)=\hat{f}(iter)-f(iter)$;

Step 3. Compute the stepsize $\varsigma(iter)$;

Step 4. Update network state according to $f(iter+1)=f(iter)+\varsigma(iter)\cdot\bar{f}(iter)$;

Step 5. Convergence check. If RMSE=$\sqrt{\left\|f(iter)-\hat{f}(iter)\right\|/\sum_{ij,m}|R_{ij}^{m}|}\le\varepsilon$, stop the algorithm and output the current flow pattern; otherwise, turn to Step 1.

In Step 3, we adopt the SRA line-search scheme to determine the step size. The SRA scheme is a modification of the method of successive average (MSA) approach to achieve a flexible stepsize sequence. It does not need to calculate the objective function or its derivative; instead, it relies on the residual errors between the current flow pattern and auxiliary flow pattern to determine the step size. When the residual error becomes larger, the SRA stepsize decreases faster; otherwise, it decreases slower. The SRA stepsize is specified by

$\varsigma(iter)=1/\kappa(iter)$,

where

$$\kappa(iter)=\begin{cases}\kappa(iter-1)+\Gamma,\Gamma>1,\text{if }\left\|f(iter)-\hat{f}(iter)\right\|\ge\left\|f(iter-1)-\hat{f}(iter-1)\right\| & (18)\\ \kappa(iter-1)+\tau,\tau<1,\text{if }\left\|f(iter)-\hat{f}(iter)\right\|<\left\|f(iter-1)-\hat{f}(iter-1)\right\|. & (19)\end{cases}$$

There are other line search schemes for determining an effective step-size, such as the golden section (Sheffi, 1985), bisection (Sheffi, 1985), quadratic interpolation (Maher, 1998), Armijo's rule (Armijo, 1966), etc. Comprehensive comparison studies refer to Chen et al. (2014) and Karoonsoontawong and Lin (2015). Note that, since the above algorithm is path-based, a separate route generation method may be required for real-world applications to avoid the path enumeration problem, such as the column generation procedure (Dantzig, 1963; Damberg et al., 1996).

5. NUMERICAL EXAMPLES

This section provides three numerical examples to demonstrate the impacts of captive mode travelers on the equilibrium network performances and the evaluation of exclusive bus lane (EBL) expansion plans. The first example uses a loop-hole network to examine the effect of mode captivity and route overlapping on network performances. The second numerical example applies the dogit-PSL MMNE model to the bi-criteria EBL line expansion evaluation problem

under two mode captivity scenarios. The third numerical example uses the Seoul network to show the applicability of the dogit-PSL MMNE model in a real-size multi-modal network.

5.1. Numerical Example I: Loop-hole Network

The first numerical example uses a multi-modal loop-hole network (Fig. 7) to investigate the impacts of mode captivity, route overlapping, scale and dispersion parameters on network performances, including system total travel time (TTT) and network emission from the managers' perspective. Three modes are considered, i.e., auto, transit, and bicycle. The auto network consists of three routes among which the first two routes overlapping on link 1. The transit and bicycle networks consist of respectively one dedicated route. The network settings are given out in Table 3. Consider an area where people's average income is relatively low; many people have no access to private cars and are captive to either transit or bicycle for their daily commuting trips. Among them, the sizes of captive transit and bicycle users are more significant than that of the captive car users, as listed in the last row of Table 3.

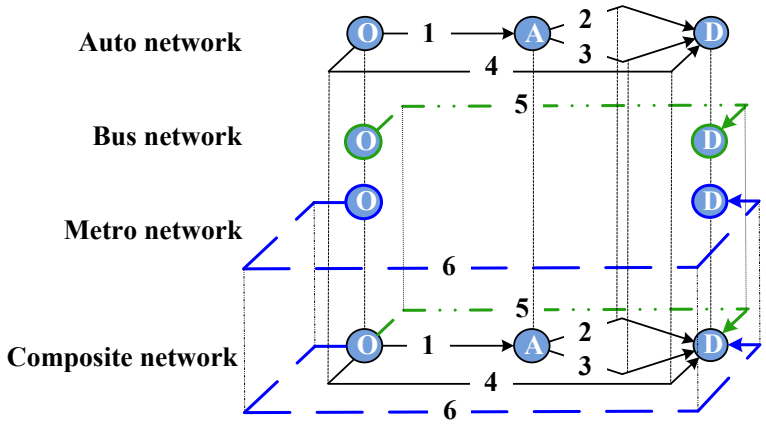

Fig. 7. The multi-modal loop-hole network

Table 3. Characteristics of the multi-modal loop-hole network

Aspects	**Auto**				**Transit**	**Bicycle**
Link	1	2	3	4	5	6
Length (kilometer)	x	18.0-x	18.0-x	18.0	18.0	25.0
FFTT (h_0^{ma}) (minute)	x	18.0-x	18.0-x	18.0	18.0	25.0
Capacity (C^{ma}) (vpm for auto; ppm for transit)	75.0	75.0	75.0	75.0	100.0	-
Exogenous attractiveness		0			2.5	7.5
Captivity parameter		0.2			0.5	0.3

In the network, the length of Link 1 (denoted by x) may vary whereby we can manipulate the route overlapping level. The lengths of Link 2 and 3 are set to 18.0-x. Thus Route 1 and 2 are equal to 18.0. The free-flow speed is set to 1 kilometer per minute on each link in each mode.

Then, the link free-flow travel time (FFTT) in each mode equals the link length. Both the auto travel time and the transit delay (results from the onboard and off-board passengers; Caliper Corporation, 2004) are assumed to follow the Bureau of Public Roads (BPR) function:

$$h^{ma} = h_0^{ma}\left(1+\alpha\left(v^{ma}/C^{ma}\right)^{\beta}\right). \tag{20}$$

where $\alpha = 0.15$ and $\beta = 4$ for auto, and $\alpha = 0.5$ and $\beta = 2$ for transit. The bicycle users have a fixed travel time of 25 minutes with an exogenous attractiveness of 7.5 units, which comes from lower travel costs, lower carbon footprints, other social benefits like monetary subsidies, and healthier travel choices. Similarly, an extra 2.5 units of exogenous attractiveness is assumed for the transit mode. The total O-D demand is set to 120 travelers per minute. The route dispersion parameter and mode scale parameter are set to 1.5 and 1.2, respectively.

Among the two network performance indicators, the network TTT is defined by

$$TTT = \sum_{m\in M}\sum_{a\in A_m} v^{ma}\cdot h^{ma}\ . \tag{21}$$

Without loss of generality, we consider the carbon monoxide (CO) emission as a major source of network emission for evaluation,

$$E = \sum_{m\in M}\sum_{a\in A} v^{ma}\cdot e^{ma}\ , \tag{22}$$

where e^{ma} is the macroscopic link-based vehicular CO emission function suggested by Wallace et al. (1998),

$$e^{ma} = 0.2038\cdot h^{ma}\cdot\exp(0.7962\cdot L^{ma}/h^{ma})\,. \tag{23}$$

Further, the transit system is assumed to run on electricity to highlight its potential in reducing CO emissions. Therefore, the CO emissions produced by the transit mode are ignored, and the auto mode becomes the unique source of CO emissions. In fact, guidelines have been published to accelerate the deployment of new energy buses in major cities in China (General Office of the State Council, 2014; Ministry of Transport et al., 2015).

5.1.1. *Network performance under different model assumptions*

This example compares the equilibrium network performances in different models, including the MNL-MNL and dogit-MNL MMNE models as base references, the MNL-PSL, and NL-PSL MMNE models to consider route and mode correlations, and the dogit-PSL MMNE model to consider mode captivity and route overlapping. The NL model is adopted to model the mode choice for having a bi-level tree structure as the dogit model. In the NL-PSL MMNE model, we group the two motorized modes (i.e., auto and transit) into one nest, while the bicycle mode has its independent nest. The nest scale parameters ϕ_{ij}^{u} ($u \in \{\text{motorized}, \text{non-motorized}\}$) are respectively set to 0.85 and 1 for the motorized and non-motorized mode nests, the dispersion

parameter for route choice (θ_{ij}^{m}) and the scale parameter for mode choice (γ_{ij}) are set respectively to 1.5 and 1.2 for all modes and O-D pairs. In the base case, the length of Link 1 (x) is set to 8 kilometers.

Table 4. Statistics of equilibrium network performances in each model

	Mode	MNL-MNL	MNL-PSL	NL-PSL	Dogit-MNL	Dogit-PSL
Modal split	Auto	42.8	40.3	38.3	36.0 (12)*	34.5 (12)
	Transit	44.2	44.7	44.4	47.6 (30)	48.1 (30)
	Bicycle	33.1	35.1	37.3	36.4 (18)	37.5 (18)
TTT		2,469.9	2,486.3	2,500.6	2,512.0	2,522.1
Emission		347.7	327.3	311.1	293.1	285.1

* () refers to the number of captive mode travelers assigned to a travel mode.

Table 4 presents the equilibrium network performances in each model. Among the MMNE models that do not consider mode captivity (i.e., MNL-MNL, MNL-PSL, and NL-PSL), the MNL-MNL MMNE model has the most significant auto users and smallest transit and bicycle users. The MNL-PSL MMNE model observes a shift from auto usage to transit and bicycle after considering route-overlapping in the auto network. Further considering the similarity of the two motorized modes, the NL-PSL MMNE model observes fewer auto users after some motorized travelers switching to the independent bicycle mode. Recall that the auto mode is assumed the only source of emission, the network emission changes in the same manner along with the size of auto users in each model. In the meantime, the network TTT shows an opposite changing momentum when compared to that of the network emission among the three models.

As for the models that consider mode captivity (i.e., dogit-MNL and dogit-PSL MMNE models), the captivity pattern plays a significant role in shaping the network performances. In these two models, the auto mode has the smallest captivity parameter among the three modes, and attracts fewer users than its counterpart in the MNL-MNL(\PSL) MMNE model and hence leads to lower network emissions. Considering route overlapping produces similar impacts on the network performances as those happened to the MNL-PSL MMNE model relative to the MNL-MNL MMNE model, thus omitted here. When compared to the NL-PSL MMNE model, we observe different impact patterns. The NL model assigns fewer users to the modes in a nest by penalizing their mode attractiveness, while the dogit model affects the modal splits by assigning more captive mode travelers to modes with more significant captivity parameters.

5.1.2. *Impacts of mode captivity and route overlapping on the network performances*

The dogit-PSL MMNE model captures two effects, i.e., captivity in the mode choice and route-overlapping in the route choice. By imposing a scalar ζ on the mode captivity parameters (i.e.,

$\hat{\eta}_{ij}^{m} = \zeta \eta_{ij}^{m}, \forall m, ij$) and varying the length x of link 1, we may connect the dogit-PSL MMNE model with some existing MMNE models demonstrated in Section 5.1.1:

(1) when ζ=0 and x>0, the dogit-PSL MMNE model degenerates to the MNL-PSL MMNE model;

(2) when ζ and x are equal to 0, the dogit-PSL MMNE model collapses to the MNL-MNL MMNE model;

(3) when ζ>0 while x=0, the dogit-PSL MMNE model reduces to the dogit-MNL MMNE model; and

(4) when ζ increases to infinity, the dogit-PSL MMNE model approaches to the multi-modal traffic assignment problem with each mode having a fixed travel demand.

To examine the coupling effects of the length x of the overlapping link and the mode captivity scalar ζ, we vary x from 0 to 16 with an interval of 2 (when x=18, Routes 1 and 2 reduce to a single route), and ζ from 0 to 3.0 with an interval of 0.5.

Fig. 8 displays the modal splits w.r.t. the combinations of x and ζ. As x increases, the auto routes 1 and 2 get more overlapped with each other, which reduces the attractiveness of the auto mode and leads to fewer auto users. When scaling up the network captivity level with a larger ζ value, the transit and bicycle modes with larger captivity parameters attract more travelers. In the meantime, it is observed that the modal split results are bounded by the MNL-PSL, Dogit-MNL and MNL-MNL MMNE models as three special cases. In Fig. 9, we present the network performance indicators under different combinations of x and ζ. Among them, the network TTT increases along with x and /or ζ; while the network emission, exhausted merely by the auto mode, declines along with larger x and /or ζ with fewer auto shares.

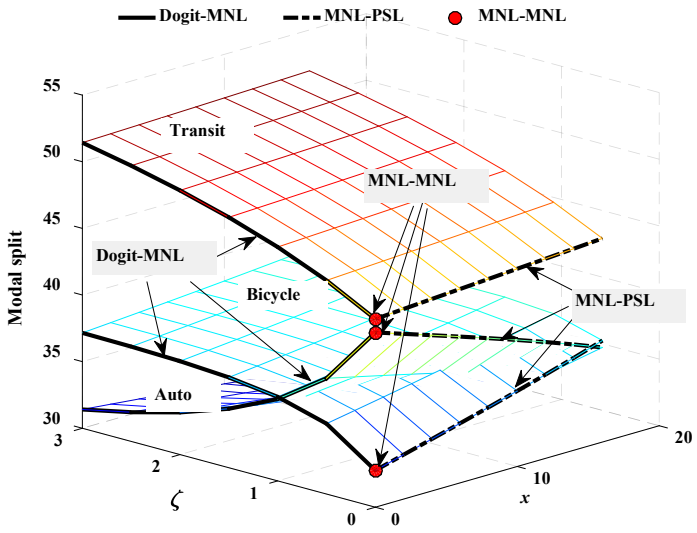

Fig. 8. Modal split w.r.t. x and ζ in the dogit-PSL MMNE model

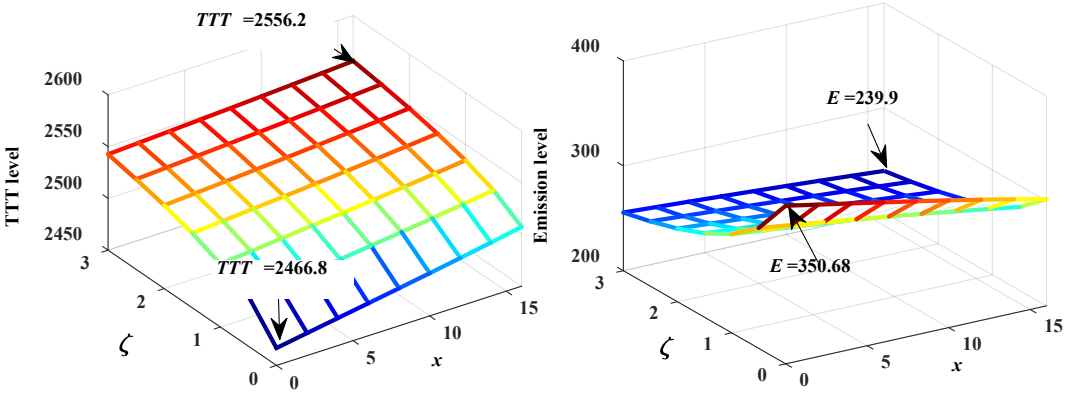

(1) Network TTT w.r.t. x and ζ (2) Network emission w.r.t. x and ζ

Fig. 9. Network performance indicators w.r.t. x and ζ in the dogit-PSL MMNE model

5.1.3. *Impacts of scale and dispersion parameters on the network performances*

In this section, we examine the impacts of mode choice scale and route choice dispersion parameters on the network TTT and total emissions. The scale parameter γ_{ij} varies from 0.6 to 1.4 with an interval of 0.1, and the dispersion parameter θ_{ij}^m varies from 1.5 to 2.3, with an interval of 0.1.

Fig. 10 presents the mode flow distributions w.r.t. combinations of θ_{ij}^m and γ_{ij}. For the auto mode, increasing the dispersion parameter θ_{ij}^m leads to lower auto mode flow, while changing the scale parameter γ_{ij} produces varied effects when θ_{ij}^m taking different values. There exists a threshold for θ_{ij}^m, below which the auto mode flow increases with γ_{ij} while decreases with γ_{ij} otherwise (see Fig. 10(1)). As shown in Fig. 10(3), a similar phenomenon occurs to the bicycle mode but with inverse changing momentum, the bicycle mode increases with θ_{ij}^m, decreases with γ_{ij} when θ_{ij}^m is smaller than the threshold while increases with γ_{ij} when θ_{ij}^m are larger than the threshold (the critical value obtained is 2.0 for the current numerical example with limited samplings). In the meantime, the transit flow shows consistent changing trends with either θ_{ij}^m or γ_{ij}, i.e., the transit flow increases with θ_{ij}^m and decreases with γ_{ij}.

Fig. 11 demonstrates the network TTT and emission changes w.r.t. combinations of θ_{ij}^m and γ_{ij}. The network TTT shows a similar trend to the bicycle mode flow, i.e., increasing with θ_{ij}^m, decreasing with γ_{ij} when θ_{ij}^m is smaller than the threshold while increasing with γ_{ij} when θ_{ij}^m is larger than the threshold. This phenomenon can be explained by that, the bicycle mode has the largest average travel time and also the largest exogenous attractiveness, its mode flow plays a significant role in determining the network TTT. Hence the network TTT has similar

trends w.r.t. θ_{ij}^{m} and γ_{ij} to the bicycle mode. At the same time, the network emission, exhausted by the auto mode only, demonstrates opposite responding patterns from the network TTT. In fact, we also examined the MNL-PSL MMNE model and observed similar phenomena regarding the mode choice distribution, network TTT, and emission changing patterns w.r.t. θ_{ij}^{m} and γ_{ij}. The results are omitted for the sake of space.

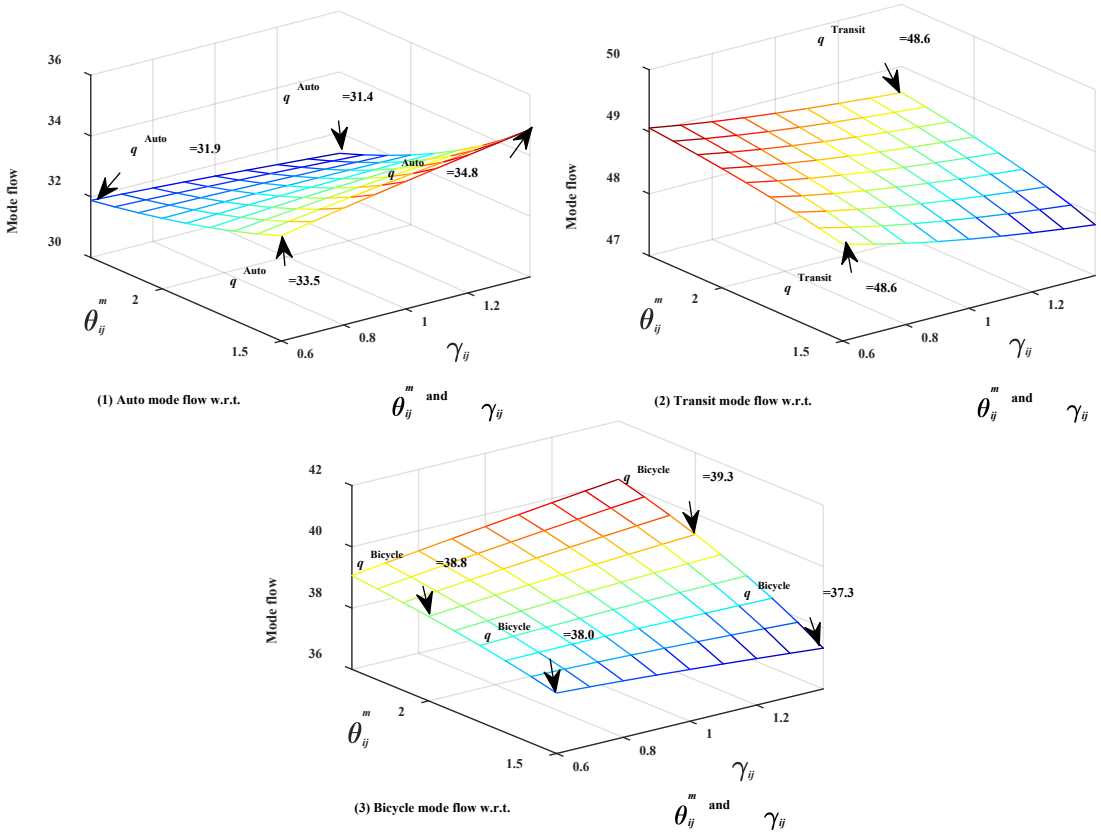

Fig. 10. Modal splits w.r.t. θ_{ij}^{m} and γ_{ij} in the dogit-PSL MMNE model

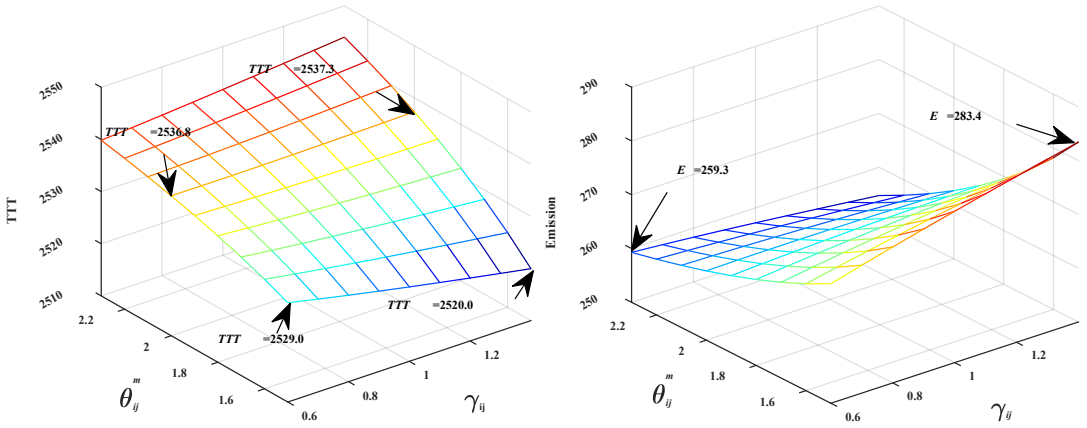

(1) Network TTT w.r.t. θ_{ij}^{m} and γ_{ij} (2) Network emission w.r.t. θ_{ij}^{m} and γ_{ij}

Fig. 11. Network performance indicators w.r.t. θ_{ij}^{m} and γ_{ij} in the dogit-PSL MMNE model

5.2. Numerical Example II: Application to the Exclusive Bus Lane Expansion Evaluation Problem

In the second numerical example, a comparative study is conducted between the dogit-PSL MMNE model and three other MMNE models (i.e., MNL-MNL, MNL-PSL, and NL-PSL) in evaluating the exclusive bus lane (EBL) expansion plans, to show the effect of ignoring mode captivity on EBL expansion decisions. Two performance measures (i.e., network TTT and emission) are used under two scenarios to demonstrate the potential impacts of misestimating mode captivity on the chance of making different EBL expansion decisions.

Setting up EBLs is regarded as a significant measure to promote bus priority, it is expected to enhance the attractiveness of public transit by improving the efficiency and service quality of the latter, thus to raise the bus ridership and to alleviate urban traffic congestion. It has received broad research interests in the literature, including topics on dynamic scheduling on EBL (Wang et al., 2018b), design of EBLs and bus frequencies (Yao et al., 2012, 2018), and evaluation method of EBL (Yao et al., 2015). However, none has considered the captive mode travelers in the EBL related studies.

5.2.1. *Basic settings*

This example aims to evaluate the EBL network expansion problem with captive mode travelers. An extended Nguyen-Dupius network (see Fig. 12) is adopted with three sub-networks, i.e., the auto, transit, and bicycle networks. The three sub-networks connect four O-D pairs, i.e., (1, 2), (1, 3), (4, 2) and (4, 3), with an O-D demand of 600, 600, 800 and 400 travelers per hour, respectively. The link characteristics of the auto network are given in Table 5. The free-flow speed on each auto link is set to 1km/min (or 60 km/hr). The transit network has one dedicated line connecting each O-D pair, which consists of EBLs with the same lengths and free-flow speeds as the co-lined auto links. All the transit links have a capacity of 800 persons per hour. Both auto and transit link travel times are assumed to follow the BPR function (Eq. 7) with $(\alpha = 0.15, \beta = 4)$ for auto and $(\alpha = 0.5, \beta = 2)$ for transit, respectively. As for the bicycle network, it has the same lengths as the co-lined auto links, but with a lower and constant travel speed of 0.6 km/min for illustration purpose. Hence, we have constant travel time on each bicycle link. The mode extra attractiveness is the same as the first numerical example.

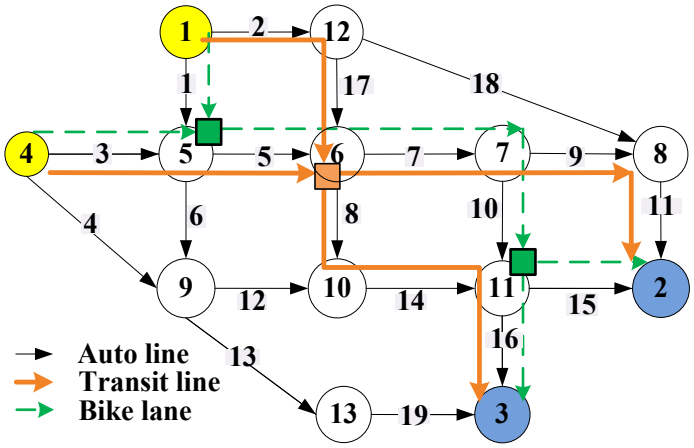

Fig. 12. The multi-modal Nguyen-Dupius network

Table 5. Link characteristics of the auto network

Link#	Distance (km)	FFTT (minute)	Capacity (vph)	Link#	Distance (km)	FFTT (minute)	Capacity (vph)
1	3.00	3.00	400	11	5.00	5.00	350
2	3.00	3.00	300	12	3.50	3.50	400
3	3.75	3.75	350	13	4.25	4.25	400
4	5.25	5.25	400	14	4.00	4.00	400
5	3.75	3.75	350	15	4.25	4.25	350
6	3.50	3.50	300	16	2.50	2.50	400
7	3.00	3.00	400	17	4.25	4.25	300
8	4.50	4.50	200	18	11.75	11.75	300
9	6.50	6.50	200	19	6.50	6.50	400
10	3.25	3.25	250				

Table 6 summarizes the two scenarios used in the second numerical example. The first scenario is used to investigate the effect of ignoring mode captivity on the EBL evaluation by comparing to three other MMNE models; while the second scenario, by comparing to the first scenario, is used to show the potential impacts of misestimating mode captivity pattern on the EBL expansion decisions. The two scenarios differ in the settings of origin and destination, which determine the mode captivity pattern between each O-D pair. In Scenario I, Origins 1 and 4 are respectively a white-collar residence area and a blue-collar residence area, while Destinations 2 and 3 are respectively an office zone and a recreation zone. In Scenario II, the roles of the two origins are switched and those of the two destinations keep unchanged. The mode captivity settings ($\eta_{ij}^{\text{Auto}}, \eta_{ij}^{\text{Transit}}, \eta_{ij}^{\text{Bicycle}}$) for each O-D pair each scenario are presented in Table 7. Generally, we assume more captive auto travelers among the white-collar residents for

both work and recreation journeys, while assuming more captive bus and bicycle riders for the blue-collar residents.

Table 6. Description of the two scenarios

	Origins	Destinations
Scenario I	Origin 1: White-collar residence area	Destination 2: Office zone
	Origin 4: Blue-collar residence area	Destination 3: Recreation zone
Scenario II	Origin 1: Blue-collar residence area	Destination 2: Office zone
	Origin 4: White-collar residence area	Destination 3: Recreation zone

Table 7. Mode captivity settings for each O-D pair in each scenario

	O-D pairs			
	O-D 1	O-D 2	O-D 3	O-D 4
Scenario I	(0.8, 0.5, 0.2)*	(0.2, 0.2, 0.1)	(0.2, 0.5, 0.3)	(0.1, 0.1, 0.1)
Scenario II	(0.2, 0.7, 0.1)	(0.2, 0.2, 0.1)	(0.8, 0.5, 0.2)	(0.1, 0.1, 0.1)

* () gives the captivity parameter vector ($\eta_{ij}^{\text{Auto}}, \eta_{ij}^{\text{Transit}}, \eta_{ij}^{\text{Bicycle}}$) for an O-D pair

In each scenario, one of the four EBL lines will be expanded under a limited budget. Hence the four EBL lines between the four O-D pairs comprise four alternative expansion plans (AEPs). Capacities of the associated bus lanes in the chosen EBL line will increase by 50 percent after the expansion operation. Other model parameters are assumed the same as the first numerical example, i.e., the MNL and PSL route choice models have a dispersion parameter of 1.5, the MNL and dogit mode choice models have a scale parameter of 1.2, and the NL mode choice model has respectively the mode and O-D specific dispersion/scale parameters of 1.5 and 1.2, the scale parameters for the motorized and non-motorized mode nests are respectively set to 0.85 and 1.

5.2.2. *Scenario I*

The mode captivity settings in scenario I are presented in Table 7. For the EBL line expansion problem, it is supposed that the government wants to promote transit usage through expanding the current EBL network to achieve a balance between transport efficiency (e.g., motorized mobility) and environmental sustainability (e.g., CO emission). Two typical network performance measures (i.e., network TTT and emission) are used for evaluating the EBL lines.

To evaluate the potential benefit of expanding an EBL line, we consider the measure changes relative to the pre-expansion cases,

$$\begin{cases} \Delta TTT_{\text{Model}}^{\text{AEP}i} = TTT_{\text{Model}}^{\text{AEP}i} - TTT_{\text{Model}}^{\text{Pre-exp}} \\ \Delta E_{\text{Model}}^{\text{AEP}i} = E_{\text{Model}}^{\text{AEP}i} - E_{\text{Model}}^{\text{Pre-exp}} \end{cases}, i = 1, \ldots, 4; \quad (24)$$

$$\text{Model} \in \{\text{MNL-MNL}, \text{MNL-PSL}, \text{NL-PSL}, \text{dogit-PSL}\}$$

where $\Delta TTT_{\text{Model}}^{\text{AEP}i}$ is the change of network TTT by expanding AEPi in the 'Model' MMNE model, $TTT_{\text{Model}}^{\text{AEP}i}$ and $TTT_{\text{Model}}^{\text{Pre-exp}}$ are the network TTTs before and after expanding EBL line between O-D pair i in the 'Model' MMNE model. Similarly, $\Delta E_{\text{Model}}^{\text{AEP}i}$ is the change of network emission by expanding AEPi in the 'Model' MMNE model, as the difference between the network emissions before and after expanding EBL line i in the MMNE model "Model" (i.e., $E_{\text{Model}}^{\text{AEP}i}$ and $E_{\text{Model}}^{\text{Pre-exp}}$).

The relative changes for each EBL AEP in the four models are displayed in Fig. 13, it is observed that $\begin{cases}(\Delta TTT,\Delta E)^{\text{AEP3}}_{\cdot} \succ (\Delta TTT,\Delta E)^{\text{AEP1}}_{\cdot} \\ (\Delta TTT,\Delta E)^{\text{AEP4}}_{\cdot} \succ (\Delta TTT,\Delta E)^{\text{AEP2}}_{\cdot}\end{cases}$ for the MNL-MNL, MNL-PSL and NL-PSL MMNE models, where $A \succ B$ means each (non-positive) component of A is strictly *smaller* than its counterpart of B, i.e., A dominates B. For the dogit-PSL MMNE model, it is observed that $\begin{cases}(\Delta TTT,\Delta E)^{\text{AEP3}}_{\text{dogit-PSL}} \succ (\Delta TTT,\Delta E)^{\text{AEP1}}_{\text{dogit-PSL}} \\ (\Delta TTT,\Delta E)^{\text{AEP3}}_{\text{dogit-PSL}} \succ (\Delta TTT,\Delta E)^{\text{AEP2}}_{\text{dogit-PSL}} \\ (\Delta TTT,\Delta E)^{\text{AEP3}}_{\text{dogit-PSL}} \succ (\Delta TTT,\Delta E)^{\text{AEP4}}_{\text{dogit-PSL}}\end{cases}$, i.e., AEP3 dominates the other three AEPs. The above observations suggested that the dogit-PSL MMNE model would support expanding AEP3, while the other three models would suggest AEPs 3 and 4 as effective options.

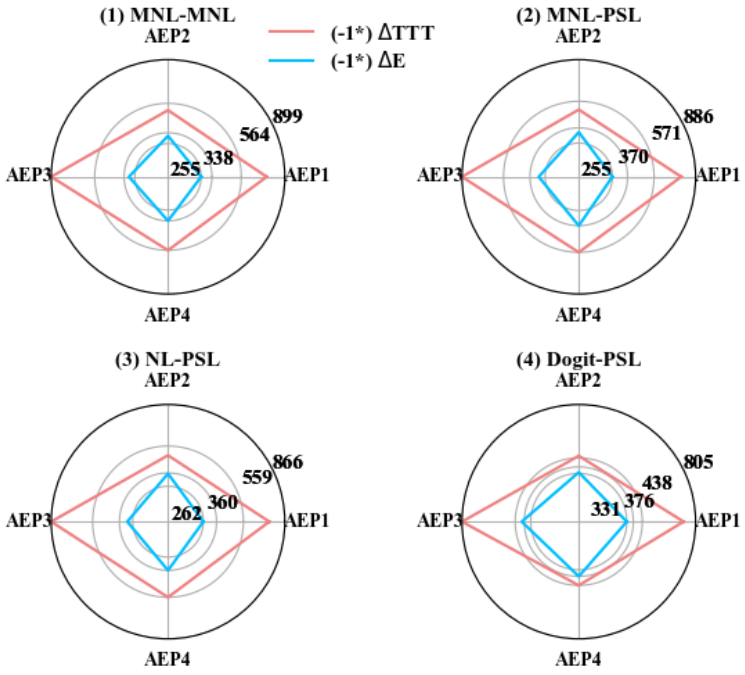

Fig. 13. TTT and emission changes for each AEP and each model

To quantify the choice probabilities of each AEP in each model, we adopt a weighted average of the *proportional* changes relative to the pre-expansion case $(\frac{\Delta TTT_{\text{model}}^{\text{AEP}i}}{TTT_{\text{model}}^{\text{Pre-exp}}}, \frac{\Delta E_{\text{model}}^{\text{AEP}i}}{E_{\text{model}}^{\text{Pre-exp}}})$ as the synthetic impact (*SI*) index of adopting AEPi

$$SI_{\text{model}}^{\text{AEP}i} = \vartheta_{\text{TTT}} \frac{\Delta TTT_{\text{model}}^{\text{AEP}i}}{TTT_{\text{model}}^{\text{Pre-exp}}} + (1-\vartheta_{\text{TTT}}) \frac{\Delta E_{\text{model}}^{\text{AEP}i}}{E_{\text{model}}^{\text{Pre-exp}}}, \quad i = 1,...,4; \\ \text{model} \in \{\text{MNL-MNL}, \text{MNL-PSL}, \text{NL-PSL}, \text{dogit-PSL}\} \tag{25}$$

where ϑ_{TTT} is a dimensionless weight parameter of network TTT ranging from 0 to 1. Without loss of generality, it is supposed that the weight parameter ϑ_{TTT} follows a uniform distribution from 0 to 1, i.e., $\vartheta_{\text{TTT}} \sim \text{U}[0,1]$.

Remark 1: Note that we use the proportional changes $\frac{\Delta TTT_{\text{model}}^{\text{AEP}i}}{TTT_{\text{model}}^{\text{Pre-exp}}}$ and $\frac{\Delta E_{\text{model}}^{\text{AEP}i}}{E_{\text{model}}^{\text{Pre-exp}}}$ to eliminate the dimension effect. One may argue that instead of proportional changes in network indices, the policymaker would be concerned about the collective network indices, i.e., network TTT and Emission. In fact, the proportional network indices $(\frac{\Delta TTT_{\text{model}}^{\text{AEP}i}}{TTT_{\text{model}}^{\text{Pre-exp}}}, \frac{\Delta E_{\text{model}}^{\text{AEP}i}}{E_{\text{model}}^{\text{Pre-exp}}})$ will produce consistent suggestions with those produced based on the aggregate network indices $(TTT, E)_{\text{model}}^{\text{AEP}i}$.

Proposition 3. *The proportional network indices* $(\frac{\Delta TTT_{\text{model}}^{\text{AEP}i}}{TTT_{\text{model}}^{\text{Pre-exp}}}, \frac{\Delta E_{\text{model}}^{\text{AEP}i}}{E_{\text{model}}^{\text{Pre-exp}}})$ *suggest a consistent dominance relationship among the AEPs with those produced by the collective network indices* $(TTT, E)_{\text{model}}^{\text{AEP}i}$.

Proof. Proposition 3 can be proved by stating that $(\frac{\Delta TTT_{\text{model}}^{\text{AEP}i}}{TTT_{\text{model}}^{\text{Pre-exp}}}, \frac{\Delta E_{\text{model}}^{\text{AEP}i}}{E_{\text{model}}^{\text{Pre-exp}}})$ has the same dominant relationship as $(TTT, E)_{\text{model}}^{\text{AEP}i}$. Suppose $(\frac{\Delta TTT_{\text{model}}^{\text{AEP}i}}{TTT_{\text{model}}^{\text{Pre-exp}}}, \frac{\Delta E_{\text{model}}^{\text{AEP}i}}{E_{\text{model}}^{\text{Pre-exp}}}) \succ (\frac{\Delta TTT_{\text{model}}^{\text{AEP}j}}{TTT_{\text{model}}^{\text{Pre-exp}}}, \frac{\Delta E_{\text{model}}^{\text{AEP}j}}{E_{\text{model}}^{\text{Pre-exp}}})$, we have from Eq. (24)

$$\begin{cases} \frac{TTT_{\text{model}}^{\text{AEP}i} - TTT_{\text{model}}^{\text{Pre-exp}}}{TTT_{\text{model}}^{\text{Pre-exp}}} \le \frac{TTT_{\text{model}}^{\text{AEP}j} - TTT_{\text{model}}^{\text{Pre-exp}}}{TTT_{\text{model}}^{\text{Pre-exp}}} \\ \frac{E_{\text{model}}^{\text{AEP}i} - E_{\text{model}}^{\text{Pre-exp}}}{E_{\text{model}}^{\text{Pre-exp}}} \le \frac{E_{\text{model}}^{\text{AEP}j} - E_{\text{model}}^{\text{Pre-exp}}}{E_{\text{model}}^{\text{Pre-exp}}} \end{cases} \rightarrow \begin{cases} TTT_{\text{model}}^{\text{AEP}i} \le TTT_{\text{model}}^{\text{AEP}j} \\ E_{\text{model}}^{\text{AEP}i} \le E_{\text{model}}^{\text{AEP}j} \end{cases} \rightarrow (TTT, E)_{\text{model}}^{\text{AEP}i} \succ (TTT, E)_{\text{model}}^{\text{AEP}j}.$$

This completes the proof. □

Remark 2: Although Proposition 3 admits a consistent dominance relationship between the proportional and collective network indices, the proportional synthetic impact $SI_{\text{model}}^{\text{AEP}i}$ may generate different choice probabilities of AEPs from those based on the aggregate indices. By adopting a relative index, we may focus on the improvements achieved by taking an EBL AEP. Besides, a proportional index can alleviate the unit effect and allow us to focus on the decision-makers' weight preferences (i.e., ϑ_{TTT}).

Fig. 14 displays the synthetic impacts of expanding AEP 3 or 4 w.r.t. ϑ_{TTT} in the four models. Generally, considering mode captivity may significantly affect the set of effective

expansion plans and hence the chance of each effective expansion plan being chosen for the operation. In the MNL-MNL MMNE model, AEP4 dominates AEP3 when ϑ_{TTT} varies from 0 to 0.3533, the reverse situation happens when ϑ_{TTT} varies from 0.3533 to 1. This means AEP4 has a 35.33 percent chance of being chosen as the expansion plan, while AEP3 takes the remaining 64.67 percent chance. Similarly, the chances of AEP4 being chosen in the MNL-PSL and NL-PSL MMNE models are 51.72 percent and 49.17 percent, respectively. However, when considering the captive mode travelers, AEP3 will dominate AEP4 across all ϑ_{TTT} values, i.e., AEP3 will be the only expansion plan being chosen in the dogit-PSL MMNE model. Hence, ignoring mode captivity may cause 35.33, 51.72, and 49.17 percent chances of making different expansion plan decisions in the MNL-MNL, MNL-PSL and NL-PSL MMNE models.

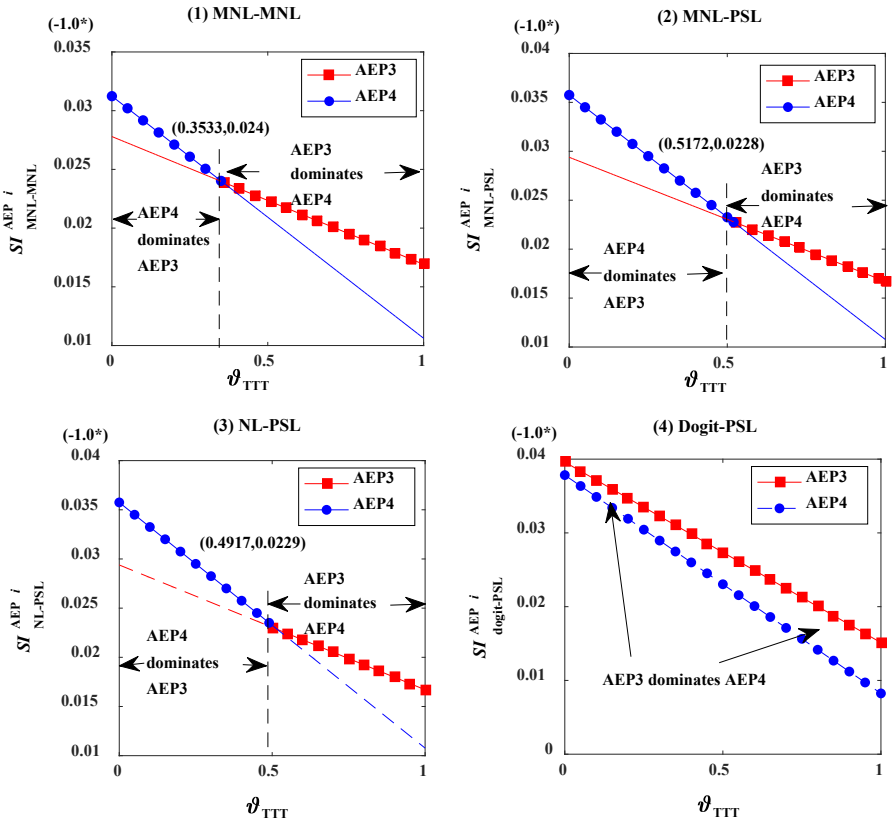

Fig. 14. Synthetic impacts of expanding AEP 3 or 4 w.r.t. ϑ_{TTT} in the four models

5.2.3. *Scenario II*

In scenario II, we switch the roles of the two origins and adjust the mode captivity parameters as listed in Table 7. O-D pair 1 has less captive auto and bicycle travelers and more captive transit users when compared with those in the scenario I, O-D pair 3 has more captive auto travelers and less captive transit and bicycle users at the same time. Other settings are the same as those in scenario I.

Table 8 presents the changes in network TTT and emission relative to the pre-expansion cases for the four AEPs. We may observe that $\begin{cases}(\Delta TTT,\Delta E)^{\text{AEP1}}_{\text{dogit-PSL}} \succ (\Delta TTT,\Delta E)^{\text{AEP4}}_{\text{dogit-PSL}} \\ (\Delta TTT,\Delta E)^{\text{AEP3}}_{\text{dogit-PSL}} \succ (\Delta TTT,\Delta E)^{\text{AEP2}}_{\text{dogit-PSL}}\end{cases}$, i.e., apart from AEP3, AEP1 is considered as another effective expansion plan.

Then, we turn to the *SI* traces w.r.t. ϑ_{TTT}. As shown in Fig. 15, AEP3 dominates AEP1 for $0 \le \vartheta_{\text{TTT}} < 0.7400$ and AEP1 dominates AEP3 for $0.7400 < \vartheta_{\text{TTT}} \le 1$, while AEP4 is dominated by both AEPs 1 and 3 for all ϑ_{TTT} values. It implies that AEPs 1 and 3 respectively have 26 percent and 74 percent chances of being chosen as the expansion plan.

Table 8. TTT and emission changes for the dogit-PSL MMNE model in Scenario II

	AEP1	AEP2	AEP3	AEP4
$\begin{pmatrix}\Delta TTT \\ \Delta E\end{pmatrix}^{\text{AEP}i}$	$-1*\begin{pmatrix}921.5311 \\ 354.6805\end{pmatrix}$	$-1*\begin{pmatrix}499.5150 \\ 361.5135\end{pmatrix}$	$-1*\begin{pmatrix}905.7760 \\ 363.1666\end{pmatrix}$	$-1*\begin{pmatrix}418.0080 \\ 341.4628\end{pmatrix}$
$\frac{\Delta TTT^{\text{AEP}i}}{TTT^{\text{Pre-exp}}}$	-0.0173	-0.0094	-0.0170	-0.0078
$\frac{\Delta E^{\text{AEP}i}}{E^{\text{Pre-exp}}}$	-0.0352	-0.0358	-0.0360	-0.0338

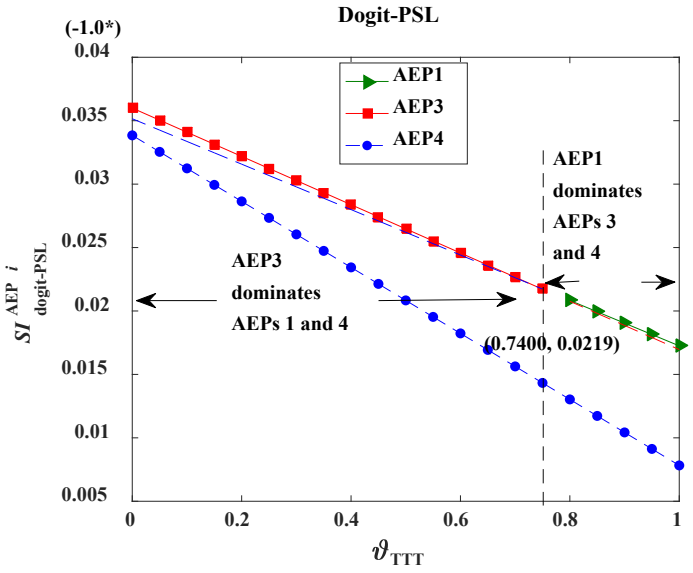

Fig. 15. Synthetic impacts of expanding AEPs 1, 3 and 4 in the dogit-PSL MMNE model

The EBL line expansion suggestions for each model in each scenario are summarized in Fig. 16. When compared to the three models without captive mode travelers, similar to the observations in Scenario I, the dogit-PSL MMNE model in Scenario II gives different effective AEP sets and also different AEP choice probabilities. The MNL-MNL MMNE model suggests a different effective AEP from the dogit-PSL MMNE model does (in Scenario II) for $\vartheta_{\text{TTT}} < 0.3533$ or $0.74 < \vartheta_{\text{TTT}} \le 1$. Similar situations happen for the MNL-PSL MMNE

model when $\vartheta_{TTT} < 0.5172$ or $0.74 < \vartheta_{TTT} \le 1$ and for the NL-PSL MMNE model when $\vartheta_{TTT} < 0.4179$ or $0.74 < \vartheta_{TTT} \le 1$. The above observations imply that the MNL-MNL MMNE model has a 61.33 percent probability of making a different AEP suggestion from the dogit-PSL MMNE model, while the MNL-PSL and NL-PSL MMNE models respectively have 77.72 percent and 75.17 percent chances of making different AEP suggestions from the dogit-PSL MMNE model. When compared to the dogit-PSL MMNE model in Scenario I, the dogit-PSL MMNE model in Scenario II suggests a different effective AEP when $0.74 < \vartheta_{TTT} \le 1$, i.e., the difference in mode captivity assumption in Scenario II causes about 26 percent chances of making a different AEP suggestion. Hence, we may conclude that misestimating the mode captivity parameters may produce a significant impact on the effective AEP set and also the AEP choice probabilities.

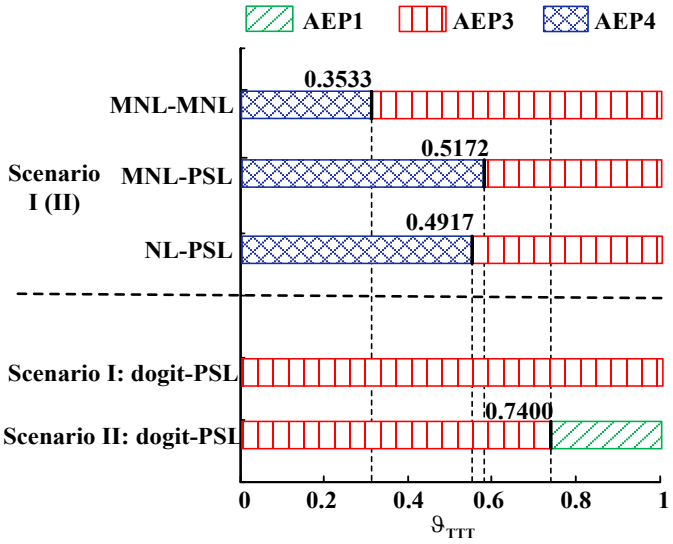

Fig. 16. Summary of AEP suggestions in each model each scenario

5.3. Numerical Example III: The Seoul Network

The third numerical example adopts the Seoul network to demonstrate the applicability of the proposed MMNE model to a large-scale multi-modal transportation network. Seoul city has the largest population in South Korea with about 9.9 million people and produces 2.9 million daily trips according to the Metropolitan Transport Association (MTA). The Seoul network contains 425 zones, 7,512 nodes, 11,154 links, and 107,434 O-D pairs. Among which, the auto mode has a total length of 2,790 km roadways, the bus mode contains 3,635 stations in 1,765 lines, the metro mode has 354 stations in 14 lines. We use the captivity parameters assumed in Ryu et al. (2018), with the sum of all captivity parameters being equal to 3.16, or a total share of 76 percent captive mode travelers without car registration (the total car registration is about 2.4 million). The mode-specific captivity parameters are set to 1.58, 0.63 and 0.95 for auto, bus and metro, respectively.

The travel cost functions for the three modes are listed as follows:

Auto: $w_{ij}^{\mathrm{C},r} = \sum_{a \in A_{ij}^{mr}} h^{\mathrm{C},a}(v^{\mathrm{C},a})$; (26)

Bus: $w_{ij}^{\mathrm{B},r} = \sum_{a \in A_{ij}^{\mathrm{B},r}} h^{\mathrm{B},a}(v^{\mathrm{B},a}) + \pi_{ij}^{\mathrm{B}}$; (27)

Metro: $w_{ij}^{\mathrm{M},r} = \sum_{a \in A_{ij}^{\mathrm{M},r}} h^{\mathrm{M},a} + \pi_{ij}^{\mathrm{M}}$. (28)

where the travel times for auto and bus are flow-dependent while that for metro is flow-independent, π_{ij}^{B} and π_{ij}^{M} are mode-specific parameters, consisting of access/egress time and fare converted to equivalent time unit. The dispersion/scale parameters for route and mode choices ($\theta_{ij}^{m}, \gamma_{ij}$) are set to (0.5, 0.2), the SRA parameters (Γ, τ) are set to (1.85, 0.05). The mode-specific exogenous attractiveness Ψ_{ij}^{m} is not considered for the sake of simplicity.

5.3.1. *Convergence characteristics*

Fig. 17 shows the root mean square error (RMSE) and step size traces under the SRA and MSA line search schemes. Comparing to the MSA-RMSE trace, which decreases smoothly in a sublinear curve, the SRA-RMSE trace decreases faster and achieves a higher accuracy level. In fact, the SRA algorithm achieved a smaller RMSE than the MSA algorithm after about 70 iterations and reached the accuracy of 10E-8 in 266 iterations, whereas the MSA algorithm failed to reach the accuracy of 10E-4 in 1000 iterations under the base settings. The SRA-RMSE trace shows faster convergence speed and experiences two drastic decreases, which can be explained by the step size traces. In the MSA step size scheme, the denominator $\kappa(iter)$ adds 1 each iteration. As a result, the step size drops very fast and decreases less than 0.02 after 50 iterations. Comparatively, the SRA step size decreases much slower by taking a small $\tau < 1$ in the denominator $\kappa(iter)$ for most iterations. When the flow difference in the current two iterations is larger than previous two consecutive iterations (i.e., Eq. (18) is satisfied), the SRA line search scheme would decrease the step size faster by adding $\Gamma > 1$ in the denominator $\kappa(iter)$ and leads to drastic drops of the SRA-RMSE at the same time.

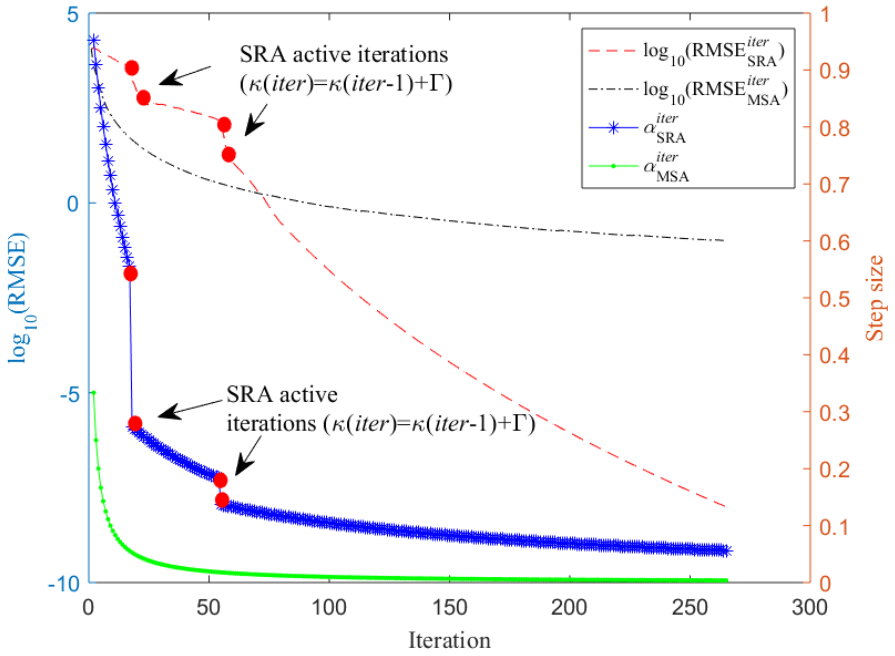

Fig. 17. RMSE and step size traces under the SRA and MSA line search schemes

Fig. 18 shows the sensitivity of the proposed solution algorithm w.r.t. different parameters (i.e., θ_{ij}^{m} and γ_{ij}, and Γ and τ). Generally, the partial linearization algorithm with the SRA line search scheme is robust with the combination of θ_{ij}^{m} and γ_{ij}. In contrast, the CPU times demonstrate higher sensitivity to the combination of Γ and τ in the SRA stepsize scheme. Particularly, it is observed that adopting a smaller τ tends to ensure higher solution efficiency. This can be explained by that, a small τ can slow down the decrease of SRA step sizes when Eq. (19) establishes, which are expected in most iterations. Then, the solution efficiency is guaranteed with a larger SRA step size sequence.

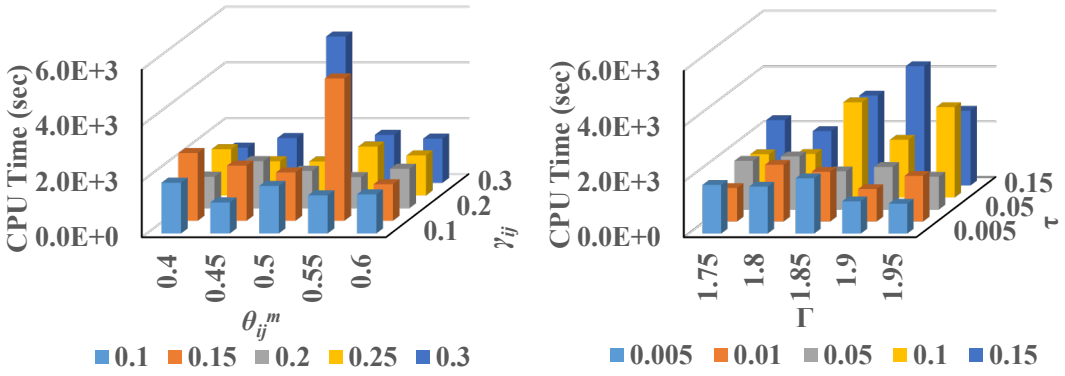

(1) Coupling effects of θ_{ij}^{m} and γ_{ij} (2) Coupling effects of Γ and τ

Fig. 18. Sensitivity of the algorithm CPU time w.r.t. different parameters (RMSE=10E-8)

5.3.2. *Impacts of mode captivity and route overlapping*

In this section, we will briefly show the mode and route flow distribution under the consideration of mode captivity and path-overlapping in the Seoul network. The dogit-MNL and MNL-PSL MMNE models are taken for comparison purposes when needed.

Fig. 19 presents the mode-specific and aggregate flow distribution in the dogit-PSL MMNE model. Among them, the auto network accommodates 44.65 percent of the total travel demand, of which 85.07 percent are captive to the car mode; for the bus network, it attracts 25.79 percent of the total travel demand with 58.73 percent of them are captive bus riders; similarly, for the rest 29.56 percent metro riders, 77.24 percent of them are captive to the metro mode. Comparing to the MNL-PSL MMNE model, the dogit-PSL MMNE model predicts more bus and metro flow after considering the 15.14 percent of total travel demand who have only access to the bus mode, and another 22.84 percent of total travel demand who are captive to the metro mode. These captive mode travelers constitute fixed travel demand for each mode, and significantly affect the modal split results. When compared to the dogit-MNL MMNE model, considering route-overlapping in the auto network reduces the attractiveness of the auto mode and leads to fewer auto drivers in the dogit-PSL MMNE model.

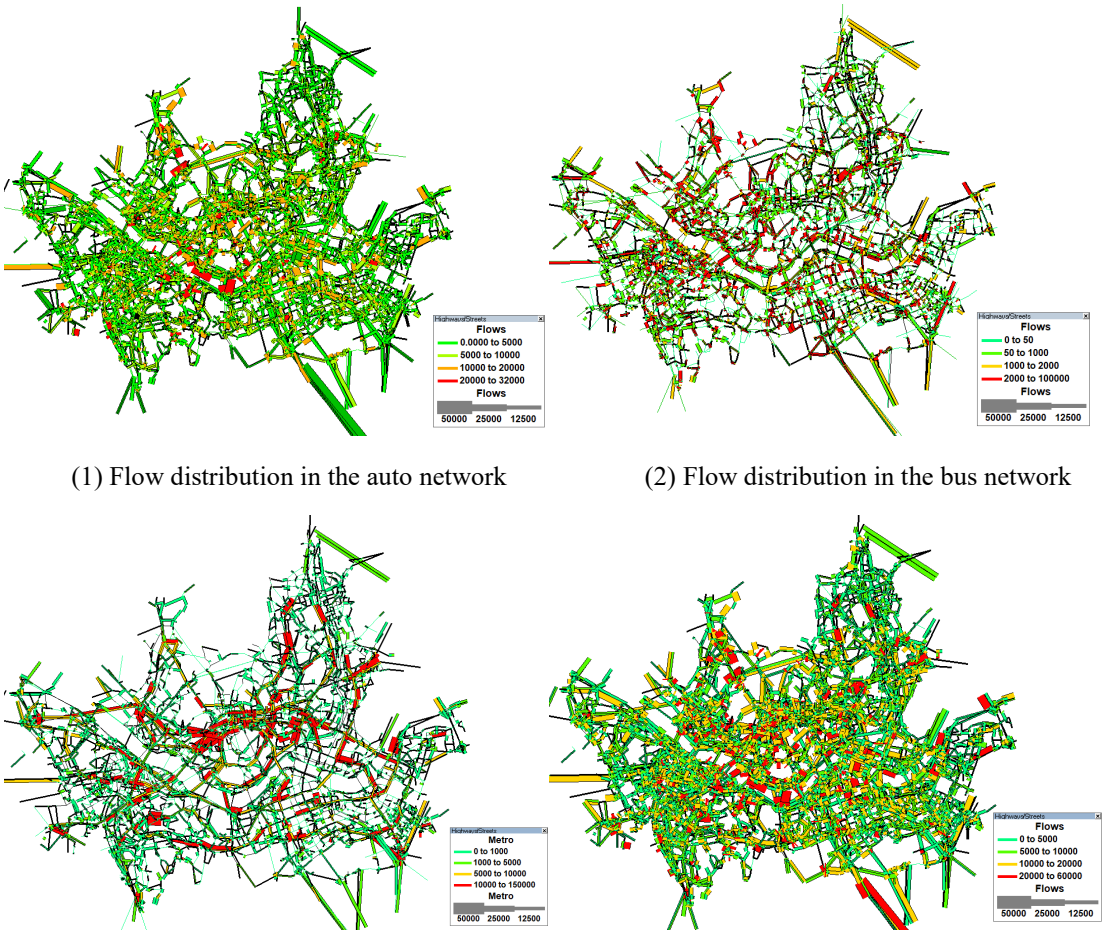

(1) Flow distribution in the auto network

(2) Flow distribution in the bus network

(3) Flow distribution in the metro network

(4) The aggregate flow distribution

Fig. 19. Mode-specific and aggregate flow distribution in the dogit-PSL MMNE model

Then, we turn to the traffic assignment results and take the auto mode for example. Fig. 20 displays the link volume/capacity (V/C) distribution in the three models. In fact, the auto link V/C distribution pattern can be connected to the modal split and traffic assignment results. As aforementioned, either considering captive mode travelers (as compared to the MNL-PSL MMNE model) or considering route overlapping in the auto network (as compared to the dogit-MNL MMNE model), would reduce the auto travel demand in the dogit-PSL MMNE model. Consequently, we may expect more links with lower V/C ratios. This happens for the dogit-PSL MMNE model when compared to the MNL-PSL MMNE model, particularly for the V/C ranges [0, 0.5) and [0.5, 1.0). However, when compared to the dogit-MNL MMNE model, there are slightly more congested auto links with higher V/C values in the dogit-PSL MMNE model, which can be explained as the synthetic effects of route overlapping effect and network topologies.

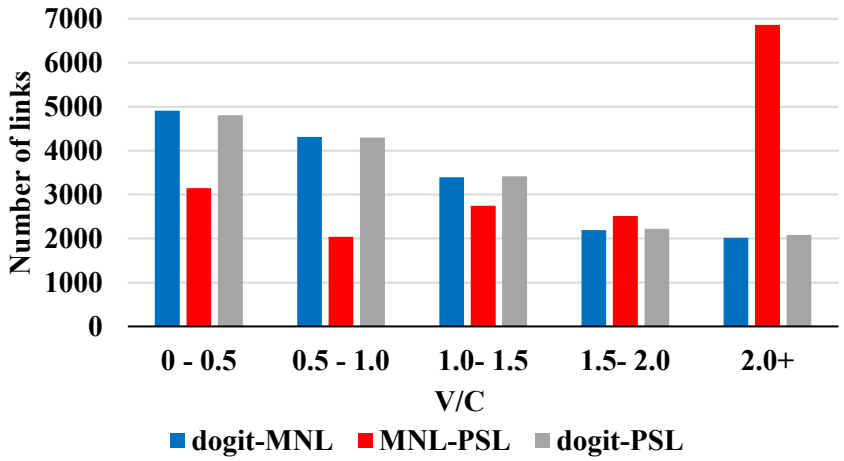

Fig. 20. Link V/C distribution in each model

6. CONCLUSIONS AND FUTURE RESEARCH DIRECTIONS

This study develops a new multi-modal network equilibrium (MMNE) model that considers captive mode travelers and route-overlapping effects, the dogit model and PSL model are respectively adopted to these ends. An equivalent MP formulation for the MMNE problem is provided, which permits the existence and uniqueness of solutions. The dogit-PSL MMNE model is applied to evaluate different exclusive bus lane expansion plans, for which a proportional two-dimension network performance indicator is developed. Numerical results under different scenario settings demonstrate that accounting for captive mode travelers would produce different equilibrium states and hence the network performance indicators, while ignorance or misestimation of mode captivity may cause substantially different evaluation of transportation policies and increase the probability of making different policy decisions.

The current research provides a preliminary effort to consider mode captivity in the combined mode-route travel choice framework, and there are many aspects deserve further investigation. First, empirical studies are required to examine the validity of the dogit-PSL MMNE model and also to estimate the mode captivity and scale/dispersion parameters. Given the available survey data, we may either take a two-stage estimation process by parameterizing the mode captivity and scale parameters as functions of independent variables or take an integrated one by fitting the dogit-PSL model to the joint mode-route choice data. Second, the study assumes a crisp definition of captivity, which is not accurate when emerging technologies largely increase the accessibility and affordability to shared mobility services (e.g., sharing bike and e-hailing service). Therefore, a possible extension of the MMNE model is to consider proportional captivity to a mode. Besides, the dogit-PSL MMNE model is built at the route-level, path-based solution algorithm together with the path generation scheme that is required for real-size networks. Efforts are merited for better computation efficiency. Recently, Ryu et al. (2014) reformulated the elastic demand network equilibrium as an excess-demand problem and resolved it with a modified the gradient projection algorithm, Kitthamkesorn et al. (2015) reformulated the MMNE problem as a traffic equilibrium problem with excess-demand which is solvable with a modified path-based gradient projection algorithm (see also Ryu et al., 2017). This encourages us to develop new algorithms out of existing ones (e.g., Chen et al., 2001; Yu et al., 2014; Zhou et al., 2014). Other efforts could be paid to develop the link-based equivalent formulation or link-based solution algorithms for the MMNE problem. Potential applications of the dogit-PSL MMNE model include evaluation of existing transportation policies, such as transit-oriented development strategies and network design optimization problems with equity considerations.

ACKNOWLEDGMENTS

This research was supported by the Research Committee of the Hong Kong Polytechnic University (Grant No. 1-ZE5T), the Research Grants Council of the Hong Kong Special Administrative Region (Grant No. 15212217), the National Natural Science Foundation of China (Grant No. 71801106, 71801105, 71871102), the Science Foundation of Ministry of Education of China (Grant No. 17YJC630150). The forth author was funded by the Korea Institute of Science and Technology Information (Grant No. K-20-L01-C06-S01). These supports are gratefully acknowledged. The comments and suggestions of three anonymous reviewers are also acknowledged.

REFERENCES

Abdulaal, M., & Leblanc, L.J. (1979). Continuous equilibrium network design models. *Transportation Research Part B,* 13(1), 19-32.

Armijo, L. (1966). Minimization of functions having continuous partial derivatives. *Pacifific Journal of Mathematics,* 16(1), 1–3.

Beimborn, E., Greenwald, M., & Jin, X. (2003). Accessibility, Connectivity, and Captivity: Impacts on Transit Choice. *Transportation Research Record,* 1835(1), 1–9.

Ben-Akiva, M., & Bierlaire, M. (1999). Discrete Choice Methods and their Applications to Short Term Travel Decisions. Handbook of Transportation Science. Springer US.

Boilé, M.P., & Spasovic, L.N. (2000). An implementation of the mode-split traffic-assignment method. *Computer-Aided Civil and Infrastructure Engineering,* 15(4), 293–307.

Caliper Corporation. (2004). TransCAD demand modeling manuals. Caliper Corporation, Massachusetts.

Cantarella, G.E. (1997). A general fixed-point approach to multimode multi-user equilibrium assignment with elastic demand. *Transportation Science,* 31(2), 107-128.

Cascetta, E., & Papola, A. (2001). Random utility models with implicit availability/perception of choice alternatives for the simulation of travel demand. *Transportation Research Part C,* 9(4), 249-263.

Chen, A., Lo, H.K., & Yang, H. (2001). A self-adaptive projection and contraction algorithm for the traffic equilibrium problem with path-specific costs. *European Journal of Operational Research,* 135(1), 27-41.

Chen, A., Ryu, S., Xu, X., & Choi, K. (2014). Computation and application of the paired combinatorial logit stochastic user equilibrium problem. *Computers & Operations Research,* 43, 68-77.

Chu, Y.L. (1990). Combined trip distribution and assignment model incorporating captive travel behavior. *Transportation Research Record*, 1285, 70-77.

Chu, Y.L. (2009). Work departure time analysis using dogit ordered generalized extreme value model. *Transportation Research Record,* 45(2132), 42-49.

Chu, Y.L. (2011). The Distribution and assignment of both compulsory and discretionary traffic. *Transportation Research Record*, 2263, 73-81.

Chu, Y.L. (2016). Automobile ownership model that incorporates captivity and proximate covariance. *Transportation Research Record,* 2563, 80-87.

Chu, Y.L. (2018). Implementation of a new network equilibrium model of travel choices. *Journal of Traffic and Transportation Engineering (English Edition),* 5(2), 105-115.

Dantzig, G.B., (1963). Linear Programming and Extensions. Princeton University Press, Princeton, NJ.

Damberg, O., Lundgren, J.T. & Patriksson, M. (1996). An algorithm for the stochastic user equilibrium problem. *Transportation Research,* 30B, 115-131.

Ergün, G., Stopher, P.R., & Al-Ahmadi, H.M. (1999). Captivity revisited. *Journal of Transportation Engineering,* 125(1), 1-7.

Florian, M. (1977). A traffic equilibrium model of travel by car and public transit modes. *Transportation Science,* 11(2), 166-179.

Florian, M., & Nguyen, S. (1978). A combined trip distribution modal split and trip assignment model. *Transportation Research,* 12(4), 241-246.

García, R., & Marín, A. (2005). Network equilibrium with combined modes: models and solution algorithms. *Transportation Research Part B,* 39(3), 223-254.

Gaudry, M.J.I. (1980). Dogit and Logit Models of Travel Mode Choice in Montreal. *The Canadian Journal of Economics,* 13(2), 268-279.

Gaudry, M.J.I. (1981). The inverse power transformation logit and dogit mode choice models. *Transportation Research Part B,* 15(2), 97–103.

Gaudry, M.J.I. (2015). The dogit story letter to Michael Florian.

Gaudry, M.J.I., & Dagenais, M.G. (1979). The dogit model. *Transportation Research Part B,* 13(2), 105-111.

Gaudry, M.J.I., & Wills, M.J. (1979). Testing the dogit model with aggregate time-series and cross-sectional travel data. *Transportation Research Part B*, 13(2), 155–166.

General Office of the State Council. (2014). Guidance of the general office of the State Council on speeding up the popularization and application of new energy vehicles (In Chinese). < http://www.gov.cn/zhengce/content/2014-07/21/content_8936.htm>

Habib, K.N., & Weiss, A. (2014). Evolution of latent modal captivity and mode choice patterns for commuting trips: A longitudinal analysis using repeated cross-sectional datasets. *Transportation Research Part A,* 66, 39-51.

Jacques, C., Manaugh, K., & El-Geneidy, A.M. (2013). Rescuing the captive [mode] user: an alternative approach to transport market segmentation. *Transportation* 40, 625–645. https://doi.org/10.1007/s11116-012-9437-2.

Karoonsoontawong, A., & Lin, D.Y. (2015). Combined gravity model trip distribution and paired combinatorial logit stochastic user equilibrium problem. *Networks and Spatial Economics,* 15(4), 1011-1048.

Kitthamkesorn, S., Chen, A., & Xu, X. (2015). Elastic demand with weibit stochastic user equilibrium flows and application in a motorised and non-motorised network. *Transportmetrica A,* 11(2), 158-185.

Kitthamkesorn, S., Chen, A., Xu, X., & Ryu, S. (2016). Modeling mode and route similarities in network equilibrium problem with go-green modes. *Networks and Spatial Economics*, 16(1), 33-60.

Kitthamkesorn, S., & Chen, A. (2017). Alternate weibit-based model for assessing green transport systems with combined mode and route travel choices. *Transportation Research Part B,* 103, 291-310.

Krizek, K., & El-Geneidy, A. (2007). Segmenting preferences and habits of transit users and non-users. *Journal of Public Transportation*, 10(3), 71-94.

Lee, M., & Cunningham, L.F. (1996). Customer loyalty in the airline industry. *Transport Quarterly*, 50(2), 57-72.

Li, Z.C., Yao, M.Z., Lam, W.H.K., Sumalee, A., & Choi, K. (2015). Modeling the effects of public bicycle schemes in a congested multi-modal road network. *International Journal of Sustainable Transportation*, 9(4), 282-297.

Liu, H.X., He, X., & He, B. (2009). Method of successive weighted averages (MSWA) and self-regulated averaging schemes for solving stochastic user equilibrium problem. *Networks and Spatial Economics*, 9(4), 485-503.

Liu Z.Y., Chen X., Meng, Q., & Kim, I. (2018). Remote park-and-ride network equilibrium model and its applications, Transportation Research Part B, 117(A), 37-62.

Maher, M. (1998). Algorithms for logit-based stochastic user equilibrium assignment. *Transportation Research Part B,* 32(8), 539–549.

Martínez, F., Aguila, F., & Hurtubia, R. (2009). The constrained multinomial logit: A semi-compensatory choice model. *Transportation Research Part B*, 43(3), 365-377.

McCarthy, P.S. (1997). The role of captivity in aggregate share models of intercity passenger travel. *Journal of Transport Economics and Policy*, 293-308.

Meng, Q., & Liu, Z. (2012). Impact analysis of cordon-based congestion pricing on mode-split for a bimodal transportation network. *Transportation Research Part C*, 21(1), 134-147.

Ministry of Transport, Ministry of Finance, Ministry of Industry and Information Technology. (2015). New energy bus popularization and application of assessment methods (Trial, in Chinese). http://zizhan.mot.gov.cn/zfxxgk/bnssj/dlyss/201511/t20151110_1924495.html

Oppenheim, N. (1995). Urban travel demand modeling. John Wiley and Sons Inc., New York.

Patriksson, M. (1994). The traffic assignment problem: Models and methods, VSP, Utrecht, Netherlands.

Polzin, S.E., Chu, X., & Rey, J.R. (2000). Density and capacity in public transit success observations from the 1995 Nationwide Personal Transportation Study. *Transportation Research Record,* 1735, 10-18.

Ryu, S., Chen, A., & Choi, K. (2014). A modified gradient projection algorithm for solving the elastic demand traffic assignment problem. *Computers & Operations Research*, 47, 61–71.

Ryu, S., Chen, A., & Choi, K. (2017). Solving the combined modal split and traffic assignment problem with two types of transit impedance function. *European Journal of Operational Research*, 257(3), 870-880.

Ryu, S., Chen, A., Wang, G.C., & Choi, K. (2018). Solving the combined modal split and traffic assignment problem with captive mode users and overlapping routes. *Asia Transport Studies*, 5(2), 224-242.

Saleh, W., & Al-Atawi, A.M. (2015). Captivity to car use in Saudi Arabia: A mixed logit model analysis. *International Journal of Engineering Research and Applications,* 5(6), 82-90.

Sheffi, Y. (1985). *Urban transportation networks: Equilibrium analysis with mathematical programming methods*. Prentice-Hall, Inc., Englewood Cliffs.

Srinivasan, K.K., Pradhan, G.N., & Naidu, M. (2007). Commute mode choice in a developing country: Role of subjective factors and variations in responsiveness across captive, semicaptive and choice segments. *Transportation Research Record*, 2038, 53-61.

Swait, J.D., & Ben-Akiva, M. (1986). Analysis of the effects of captivity on travel time and cost elasticities. *In: Proceedings of 1985 International Conference on Travel Behaviour*. VNU Science Press, Noordwijk, 119-134.

Swait, J.D., & Ben-Akiva, M. (1987). Empirical test of a constraint choice discrete choice model: Mode choice in Sao Paulo, Brazil. *Transportation Research Part B*, 21(2), 103-115.

Szeto, W.Y., Jaber, X., & Wong, S.C. (2012). Road network equilibrium approaches to environmental sustainability. *Transport Review*, 32(4), 491-518.

Transport Department. (2018). The annual traffic census 2017. TSSD Publication No. 18CAB1.

Van Exel, N.J.A., & Rietveld, P. (2001). Public transport strikes and traveler behavior. *Transport Policy*, 8(4), 237-246.

Venter, C. (2016). Are we giving BRT passengers what they want? User preference and market segmentation in Johannesburg. *Southern African Transport Conference*.

Wallace, C.E., Courage, K.G., Hadi, M.A., & Gan, A.G. (1998). TRANSYT-7F user's guide. University of Florida, Gainesville.

Wang, H., Lam, W.H.K., Zhang, X.N., & Shao, H. (2015). Sustainable transportation network design with stochastic demands and chance constraints. *International Journal of Sustainable Transportation*, 9(2), 126-144.

Wang, J., Peeta, S., He, X., & Zhao, J. (2018a). Combined multinomial logit modal split and paired combinatorial logit traffic assignment model. *Transportmetrica A,* 14(9), 737-760.

Wang, X., Zheng, F., Zheng, J., Liu, X., & Liu, H. (2018b). An operation scheme for dynamic sharing of exclusive bus lanes: Modeling and evaluation. T*he 97th Annual Meeting of the Transportation Research Board,* Washington DC, United States.

Williams, H.C.W.L., & Ortuzar, J.D. (1982). Behavioural theories of dispersion and the misspecification of travel demand models. *Transportation Research Part B Methodological,* 16(3), 167-219.

Wu, Z.X., & Lam, W.H.K. (2003). A combined modal split and stochastic assignment model for congested networks with motorized and non-motorized modes. *Transportation Research Record*, 1831, 57-64.

Yang, C., Chen, A., & Xu, X. (2013). Improved partial linearization algorithm for solving the combined travel-destination-mode-route choice problem. *Journal of Urban Planning and Development,* 139(1), 22-32.

Yao, J., Cheng, Z., Shi, F., An, S., & Wang, J. (2018). Evaluation of exclusive bus lanes in a tri-modal road network incorporating carpooling behavior. *Transport Policy,* 68, 130-141.

Yao J., Shi, F., An, S., & Wang, J. (2015). Evaluation of exclusive bus lanes in a bi-modal degradable road network. *Transportation Research Part C*, 60, 36-51.

Yao, J., Shi, F., Zhou, Z., & Qin, J. (2012). Combinatorial optimization of exclusive bus lanes and bus frequencies in multi-modal transportation network. *Journal of Transportation Engineering,* 138(12), 1422-1429.

Yu, Q., Fang, D., & Du, W. (2014). Solving the logit-based stochastic user equilibrium problem with elastic demand based on the extended traffic network model. *European Journal of Operational Research,* 239, 112-118.

Zhou, B., Li, X., & He, J. (2014). Exploring trust region method for the solution of logit-based stochastic user equilibrium problem. *European Journal of Operational Research,* 239, 46-57.